CRADA Final Report Form

Date: March 11, 2020

PI: Marcus Day

CRADA AWD No.: AWD00002192 **CRADA FP No.:** FP00005090

LBNL Report Number: _____

OSTI Number: _____ *(SPO to add)*

1. Parties: Alzeta Corporation
   (Identify Parties to the CRADA)

2. Title of the Project: Improving Gas Reactor Design with Complex Non-Standard Reaction Mechanisms in a Reactive Flow Model

3. Summary of the specific research and project accomplishments:

   Fluorinated gases are critical to a number of high-technology industries including semiconductor manufacturing and related processes such as flat panel display, LED, and photovoltaic manufacturing. These fluorinated gases have very high global warming potentials (GWPs) and, unfortunately are chemically very stable, in some cases lasting for thousands of years in the atmosphere. For environmental reasons, it is imperative that the release of these gases be minimized, but existing methods to destroy them requires a significant amount of energy. The goal of this project was to develop a more energy efficient method of destroying these high GWP gases using computational fluid dynamics, but the computational requirements are significant. In this project, we bring together resources available at the national labs, including high-performance computing hardware and modern computational methods, in order to explore an industrially important problem with key environmental and economic impact.

   In this project, we examined the state-of-the-art models for the physical processes involved, and made subtle changes to arrive at alternative formulations considerably better suited for computation and study. We examined several representative scenarios and developed a set of analyses techniques and tools that could be used to explore the systems in much greater detail.

   This exploratory project has demonstrated to ALZETA that HPC can indeed provide a unique view into their complex engineering problem - one that is simply inaccessible by any other means. The tools allow us to explore the details of the chemical process, and allow one to construct ``what-if'' scenarios to address shortcomings of the physical device in its current

operating modes. However, as with many sources of completely new information, many new questions are illuminated with this capability. It will take considerable time, effort and experience before we learn to probe the solutions, pose operating scenarios and confirm modifications to the device that lead to real engineering advances.

4. Deliverables:
   Original schedule of tasks appears below. LBNL provided code, simulations, analysis tools. ALZETA provided data, original chemistry models, interpretation of analysis results, and system designs. All tasks were delivered on time by both parties.

	Month											
Task and Description	1	2	3	4	5	6	7	8	9	10	11	12
Task 1. Code and Input Data Preparation												
Task 2. Model Validation												
Task 3. Parametric Simulation of Critical Design Parameters												
Task 4. Analysis of Task 3 Results, Refined Parametric Simulations												
Task 5. Specification of New System Design												

5. Identify (list below) and attach all publications or presentations at conferences directly related to the CRADA: None

6. List of Subject Inventions and software developed under the CRADA: None

7. A final abstract suitable for public release:

Fluorinated gases are critical to a number of high-technology industries including semiconductor manufacturing and related processes such as flat panel display, LED, and photovoltaic manufacturing. These fluorinated gases have very high global warming potentials (GWPs) and, unfortunately are chemically very stable, in some cases lasting for thousands of years in the atmosphere. For environmental reasons, it is imperative that the release of these gases be minimized, but existing methods to destroy them requires a significant amount of energy. The goal of this project was to develop a more energy efficient method of destroying these high GWP gases using computational fluid dynamics, bringing together resources available at the national labs, including high-performance computing hardware and modern computational methods, in order to explore an industrially important problem with key environmental and economic impact. This exploratory project has demonstrated that HPC can indeed provide a unique view into a complex engineering problem - one that is simply inaccessible by any other means. The tools allow one to explore the details of the chemical process, and construct ``what-if'' scenarios to address shortcomings of the physical device in its current operating modes. However, as with many sources of completely new information, many new questions are illuminated with this capability. It will take considerable time, effort and experience before we learn to probe the solutions, pose operating scenarios and confirm modifications to the device that lead to real engineering advances.

8. Benefits to DOE, LBNL, Participant and/or the U.S. economy.

   The targeted industries (the high technology semiconductor, flat panel display, LED, and photovoltaic manufacturing industries) are very important economically to the U.S., but are not typically regarded as large energy users. In recent years, there has been increased awareness of the energy usage and emission from these high technology fabs. The U.S. EPA now has a "Greenhouse Gas Reporting Rule," requiring the largest facilities to report their GHG emissions. In addition, some of the larger facilities now qualify as major sources due their emissions of a combination of criteria pollutants. The semiconductor industry in general is focusing on sustainability, with one example of this being the Sustainable Manufacturing Forum and the 2016 Semicon West trade show sponsored by Semi, the semiconductor industry trade association. A specific target in this project is to reduce the energy required to destroy PFCs by one-third relative to the current state of the art. There are thousands of these types of devices in use in fabs worldwide, with a large fraction in the US. Since environmental regulations are less severe in many parts of the world, energy efficient and cost-effective solutions in the U.S. will help us maintain our global competitiveness.

   Outside of our targeted application, reactive flow modeling is critical to a number of other U.S. industries, many of which are very energy intensive and many of which could likely benefit from improvements in HPC when applied to reactive flow modeling.

9. Financial Contributions to the CRADA:

DOE Funding to LBNL	$300,000
Participant Funding to LBNL	$0
Participant In-Kind Contribution Value	$60,000
Total of all Contributions	$360,000

Improving Gas Reactor Design With Complex Non-standard Reaction Mechanisms in a Reactive Flow Model

LBL Staff: Valentina Ricchiuti, Marc Day (PI)

ALZETA Staff: John Sullivan, Michael Silberstein, Justin Legg

Final Report
March 11, 2020

Contents

List of Figures

List of Tables

1 Introduction

Fluorinated gases are critical to a number of high-technology industries including semiconductor manufacturing and related processes such as flat panel display, LED, and photovoltaic manufacturing. These fluorinated gases have very high global warming potentials (GWPs) and, unfortunately are chemically very stable, in some cases lasting for thousands of years in the atmosphere. For environmental reasons, it is imperative that the release of these gases be minimized, but existing methods to destroy them requires a significant amount of energy. The goal of this project is to develop a more energy efficient method of destroying these high GWP gases. Due to the complexity of the abatement process, computational fluid dynamics (CFD) can be a valuable tool, but the computational requirements are significant. In this project, we bring together resources available at the national labs, including high-performance computing hardware and modern computational methods, in order to explore an industrially important problem with key environmental and economic impact.

2 Configuration

In this project, we investigate a "burn-wet" type reactor produced by the company ALZETA for the purposes of CF_4 abatement via high-temperature combustion. Figure 1 shows a schematic of the ALZETA reactor along with the axisymmetric representation of it we have used in our computational study. In this reactor a stream of "process gases" (e.g., CF_4 + CH_4 + air) is injected through the top boundary of the reactor; three different configurations have been investigated for the process gases: single jet, concentric nozzles and porous top wall, as shown in Figure 1c, 1d and 1e, respectively. A porous ring "main burner" surrounds the top section of the reactor side walls, and supports a premixed flame along the inner surface of the vessel. The side walls below the porous burner are water-cooled, and water spray injectors cool the exiting product stream. In this configuration, hot gases converge radially on the process stream and ignite the contained fuel, creating the extreme enviroment necessary to break the strong bonds of the CF_4 molecules. As the flow proceeds down the reactor, the primary goal of the device is to ensure that the fluorine radicals generated in this process will *not* reform CF_4, but rather will end up in HF molecules. While HF gas is extremely toxic, it is relatively simple to remove in a subsequent chemical "scrubber" device that is attached to the bottom of the burn-wet reactor.

The chemical model describing this system is discussed in Section 4. It combines

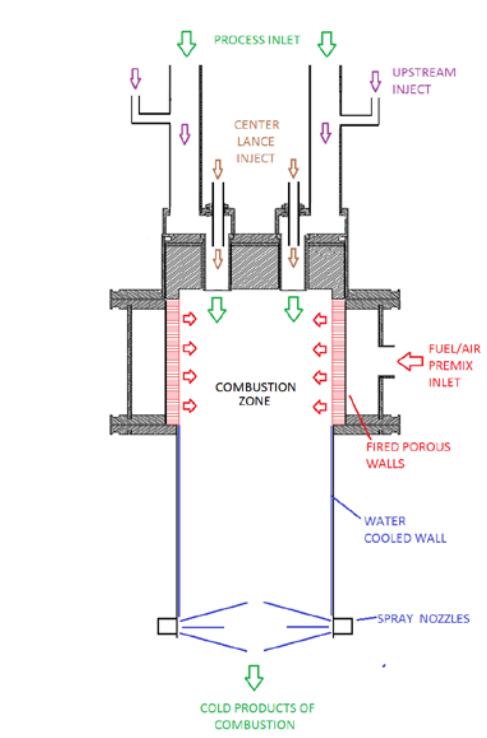

(a) Schematic

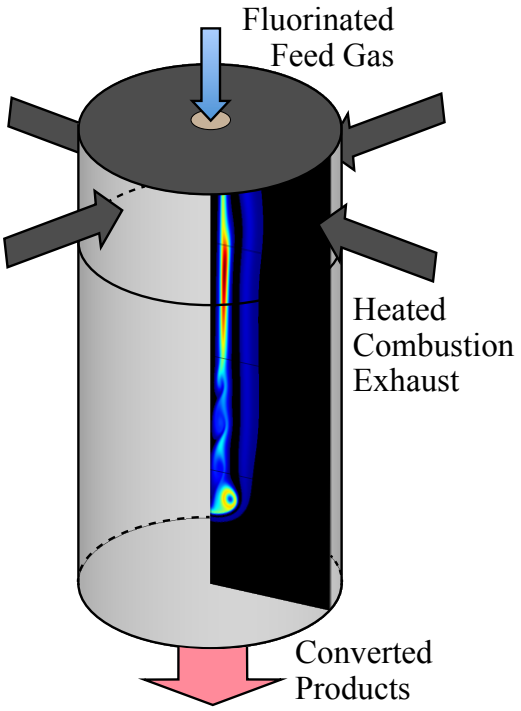

(b) Axisymmetric model (with representative evolving solution)

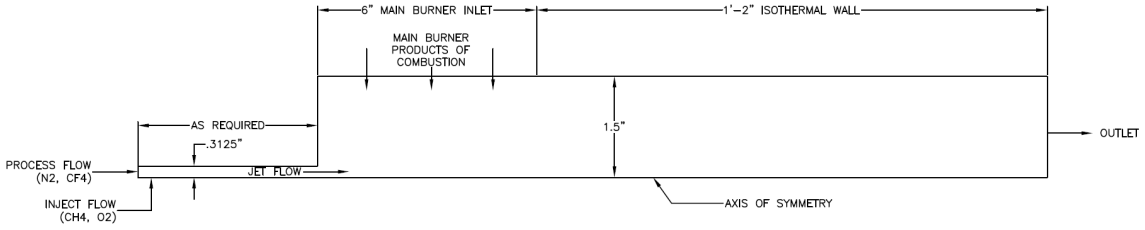

(c) Relevant dimensions - Geometry A

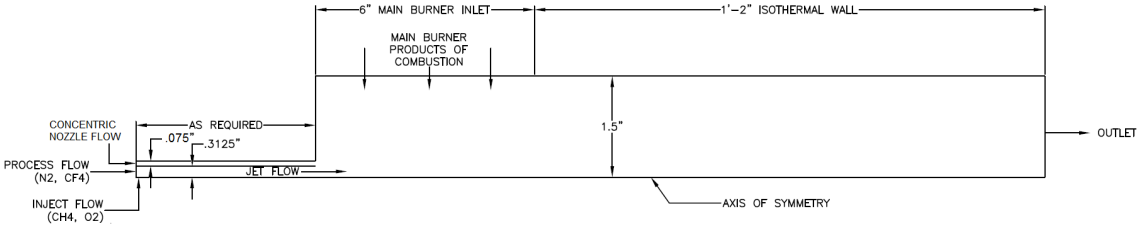

(d) Relevant dimensions - Geometry B

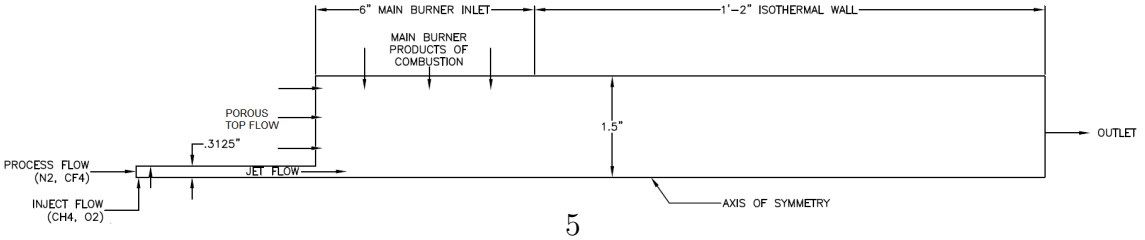

(e) Relevant dimensions - Geometry C

Figure 1: ALZETA reactor

the details necessary to describe both the combustion of methane and the reaction chemistry of fluorine. In addition to being a relatively large model, it exhibits an extremely broad range of time scales, resulting in considerable complications when used in coupled CFD calculations. Prior to this study, the model was only successfully used in extremely simplified computational configurations, including point-reactors and 1D flame idealizations. ALZETA also attempted to incorporate the model into multidimensional simulations using the reacting flow modules in OpenFoam, but the resulting numerical time step restrictions rendered practical use impossible. Without additional help, ALZETA had no viable method of simulating this device. Yet, because of the geometry of the system, very little is known about the details of the reactions within the vessel, and thus there was very little information on which to base any reasonable optimization strategy. As a result, the device is run in an "over-firing" mode, consuming a significant amount of fuel and resources in order to guarantee elimination of CF_4.

In Section 3.1 we summarize the salient aspects of the advanced numerical model, PeleLM, that we brought to bear on this system. PeleLM solves the reacting flow equations specialized to the low Mach number regime (appropriate here since the flow velocities are considerably lower than acoustic propagation speeds within the vessel), and because of the way PeleLM iteratively couples the various physical process, is capable of much larger time steps than traditional CFD codes. In Section 4 we discuss aspects of the chemical model relevant to the flow solver and the chemical objective here. Finally, in 5 we present some of the early findings and suggest directions for future work.

3 Numerical model

3.1 PeleLM and the low Mach number regime

A broad range of flow phenomena occur under conditions where advective transport is considerably slower than the local speed of sound: incompressible and inelastic hydrodynamics, atmospheric combustion, stellar hydrodynamics, etc. In such systems, it can be shown that acoustic waves transport very little energy, and thus have minimal effects on the flow evolution. A generic flow solver code could be used to simulate such conditions, but would be severely limited by the need to evolve fast-moving pressure disturbances that have no significant impact on the solution. As an alternative, this scale separation can be exploited to construct an approximate model where acoustic phenomena are entirely eliminated analytically. PeleLM is a finite-volume fluid solver for reacting flows in this low Mach number regime.

PeleLM was developed at LBNL, and is built upon the AMReX software framework for block-structured adaptive mesh refinement. It incorporates community-standard parameterized models for thermodynamics, detailed transport and Arrhenius reaction chemistry [1]. Additionally, the integration schemes in PeleLM are designed to iteratively couple the various physical processes that represent "fast" physics, with respect to advective transport. The low Mach number model, together with this coupling procedure, allows extremely large numerical time steps compared to those taken by generic compressible reacting flow solvers. PeleLM is implemented using a solution-adaptive approach to mesh generation, and executes efficiently on massively parallel computing hardware. PeleLM represents a uniquely efficient reacting flow simulation tool.

3.2 The low Mach number equations set

In the low Mach number regime, the speed of the fluid U is everywhere much smaller than the speed of sound, a; i.e., the Mach number $M = U/a \sim 0.1$, is a small parameter. To analyze this situation formally, we decompose the total pressure field as the sum of a spatially uniform value, p_0, and a perturbation, $\pi(\mathbf{x}, t)$,

$$p(\mathbf{x}, t) = p_0 + \pi(\mathbf{x}, t) \tag{1}$$

and use asymptotic analysis beginning with the reacting Navier-Stokes equations in order to estimate the magnitude of the various contributions. It has been shown that under conditions satisfied by laboratory-scale open combustion devices, $\pi/p_0 \sim \mathcal{O}(M^2)$, and π becomes independent of the thermodynamic state of the fluid. In this regime, π acts as a Lagrange multiplier that is consistent with the evolving flow field. p_0 becomes independent of space and time. The resulting set of equations that express conservation of species mass, enthalpy and momentum in the low Mach number limit [2] are given by:

$$\frac{\partial(\rho Y_m)}{\partial t} = -\nabla \cdot (\boldsymbol{U}\rho Y_m) - \nabla \cdot \boldsymbol{\Gamma}_m + \dot{\omega}_m \qquad m = 1 : N \tag{2}$$

$$\frac{\partial(\rho h)}{\partial t} = -\nabla \cdot (\boldsymbol{U}\rho h) + \nabla \cdot \lambda \nabla T - \sum_m \nabla \cdot (h_m \boldsymbol{\Gamma}_m) \tag{3}$$

$$\rho \frac{\partial \boldsymbol{U}}{\partial t} = -\rho \boldsymbol{U} \cdot \nabla \boldsymbol{U} - \nabla \pi + \nabla \cdot \tau \tag{4}$$

where N is the total number of species, ρ is the density, Y_m is the mass fraction of species m, $\boldsymbol{U}$ is the fluid velocity, $\boldsymbol{\Gamma}_m$ is the diffusive flux of species m, $h = \sum_m (Y_m h_m)$ is the total enthalpy with $h_m(T)$ the enthalpy of species m, $\dot{\omega}_m$ is the production rate of species m due to chemical reactions, and λ is the thermal

conductivity of the mixture. Ignoring bulk viscosity terms, the stress tensor in the momentum equation 4 is defined as:

$$\tau = \mu\left[\nabla \boldsymbol{U} + (\nabla \boldsymbol{U})^T - \frac{2}{3}\mathcal{I}(\nabla \cdot \boldsymbol{U})\right] \tag{5}$$

where $\mu(Y_m, T)$ is the dynamic shear viscosity and $\mathcal{I}$ is the identity tensor. Evolution of this approximate system allows a $\sim 1/M$ increase in numerical time step size, compared with that of a fully compressible method.

Note that these evolution equations are closed by an equation of state. For this work, we assume a mixture of ideal gases:

$$p_0 = \rho R_{mix} T = \rho \frac{R_u}{\overline{W}} T = \rho R_u \sum_m \frac{Y_m}{W_m} \tag{6}$$

where $\overline{W}$ is the mean molecular weight of the mixture, W_m is the molecular weight of species m and R_u is the universal gas constant. Also, there are several additional constraints implicit in this formulation. Since neither species diffusion nor chemistry redistribute total mass, $\sum_m \boldsymbol{\Gamma}_m = 0$ and $\sum_m \dot{\omega}_m = 0$. Using the definition of mass fraction, $\sum_m Y_m = 1$, the continuity equation can be derived summing up the species continuity equations:

$$\frac{\partial \rho}{\partial t} + \nabla \cdot (\rho \boldsymbol{U}) = 0 \tag{7}$$

In this work, we assume a mixture model for species diffusion:

$$\boldsymbol{\Gamma}_m = \rho Y_m \boldsymbol{\mathcal{V}}_m\,, \qquad \boldsymbol{\mathcal{V}}_m = -\Upsilon_m\, \boldsymbol{d}_m \tag{8}$$

where $\boldsymbol{\mathcal{V}}_m$ defines the diffusion velocity of species m. The transport properties of this system are evaluated using EGLIB [3], in terms of the "flux diffusion vector" $\Upsilon_m = \frac{W_m}{\overline{W}}\mathcal{D}_m$ and the diffusive driving force, $\boldsymbol{d}_m$. EGLIB provides $\mathcal{D}_m(Y_k, T)$, based on a mixing rule that combines the multispecies binary coefficients of all species, k. EGLIB also provides μ and λ. Ignoring Dufour, Soret and barodiffusion terms, the diffusion driving force becomes $\boldsymbol{d}_m = \nabla X_m$, where X_m is the mole fraction of species m.

3.3 Overview of the PeleLM time step

PeleLM implements a complex, iterative predictor-corrector strategy to advance the low Mach system of conservation equations. To facilitate the large time steps afforded by the low Mach number model, time-implicit solvers are use to advance the

diffusion physics and reaction dynamics separately, and are coupled to the time-explicit treatment of advection. The iteration is based loosely on a spectral-deferred correction strategy, where each term is advanced with a lagged approximation of the other terms in the form of a time-dependent auxiliary forcing. The diffusion advance resembles a generalized Crank-Nicolson step, with a correction to ensure discrete conservation. The reactions are integrated with a stiff ODE solver for robustness. The advection is advanced with a high-resolution fractional step approach that employs a density-weighted approximate projection to ensure the flows satisfies the divergence constraint. The PeleLM integration scheme is embedded in a parallel adaptive mesh refinement framework based on a hierarchical system of rectangular grid patches. The integration of finer levels in the hierarchy are sequenced with a subcycling approach, where each level is advanced with a time step appropriate to its grid spacing. When adjacent levels in the hierarchy reach the same time, a synchronization step is applied to ensure conservation and consistency across levels. Refinement levels are static during their time step, but are redistributed at user-specified intervals in order to satisfy refinement criteria that may evolve with the dynamic solution. This recursive adaptive integration algorithm is second-order accurate in space and time, and discretely conserves species mass and enthalpy.

Implementation of the iterative adaptive projection-based time step makes efficient use of distributed-memory parallel computing architectures; a dynamic load balancing algorithm accomodates the heterogeneous and time-dependent workload associated with chemical kinetics near the evolving flame surface, as localized patches of grid refinement are created and destroyed during the simulation. The reader is referred to [2], and subsequent enhancements [4, 5] for additional details of the low Mach number model and its adaptive implementation.

4 Reactions mechanism and path diagrams

The "reaction mechanism" is the combined specification of thermodynamic relationships (such as temperature-dependent parameterization of species specific heats), transport coefficient functions, and a network of detailed Arrhanius kinetic reactions. Our intial starting point was a mechanism provided by the ALZETA staff that included 72 species and 518 reactions. The model was assembled from two different sources:

- GRI-3.0 (53 species, 325 reactions) [6], describing the combustion of methane and subsequent formation of nitrogen-based emissions
- 0-carbon and 1-carbon reaction subset (19 species, 193 reactions) describing

fluorine combustion, as obtained from NIST [7]

Early in this project, considerable efforts were devoted to characterize this kinetic model, and to successfully incorporate it into PeleLM. It is important to stress that this type of detailed model for fluorine and carbon chemistry is not widely used in high-resolution, time dependent reacting flow calculations. The models include a number of chemical subprocess which exhibit evolution dynamics over an extremely broad range of timescales – some far shorter than the advection phyics evolved by PeleLM. A key result of this early analysis was the identification of a subset of the reactions in the model which drive the smallest of time scales observed, yet were also identified as sources of considerable uncertainty. Through careful analysis and an extensive literature search, we were able to manually adjust the parameters associated with these reactions within the bounds of published uncertainties to obtain a new model that, while still providing acceptable predictions for measured experimental data, led to far less extreme variations in observed chemical reaction time scales.

In order to identify the key chemical processes that convert CF_4 to HF in the context of the flow reactor fluid environment, a reaction path analysis was performed based on a range of simple idealized steady 1D counterflow diffusion flame solutions, and later, based on a set of 2D premixed flames. Based on these flames, we identified the dominate pathways the F atoms take through chemical space from CF_4 to HF. One important use of this information is as a quantitative measure of space and time resolution requirements for the multidimensional coupled simulation. That is, what are the cell size and time steps required of PeleLM in order to capture the key chemical pathways, and what are the degradation modes as we reduce the resolution? This provides a meaningful approach to computational convergence analysis that focuses on the end goals of the simulation, and can be contrasted to typical approaches that involve norms over the domain of various state quantities. A second outcome of this analysis is that once we have identified the most important chemical pathways of this system, we can ask whether simpler models could reproduce the results at a fraction of the cost. In fact, we used our analysis to verify that a simpler model, based on DRM19 (21 species, 84 reactions), rather than Gri-30, was able to capture the key fluorine pathways. **Note that this finding is key discovery of the work!** DRM19, coupled with the NIST fluorine mechanism, resulted in a major reduction in the stiffness of the overall chemical model, while also dramatically reducing the number of species that had to be evolved by PeleLM. Thus, we were able to rigorously justify the use of a model that required orders of magnitude less computing resources.

Table 1 summarizes the initial conditions for the different types of flames considered; results from these simulations show that:

	Composition	Temperature	Inlet velocity	Software
Counterflow diffusion flame	Fuel: 95% CH_4 + 5% CF_4 Ox: product of CH4-air premixed flame ($\phi = 0.558$)	$T_f = 350K$ $T_{ox} = 1588K$	$u_f = 0.3\frac{m}{s}$ $u_{ox} = 0.3\frac{m}{s}$	Cantera
Counterflow diffusion flame	Fuel: 95% CH_4 + 5% CF_4 Ox: air	$T_f = 400K$ $T_{ox} = 400K$	$\dot{m}_f = 0.72\frac{kg}{m^2 s}$ $\dot{m}_{ox} = 0.35\frac{kg}{m^2 s}$	CCSE's RPD
Premixed flame	(95% CH_4 + 5% CF_4)+air Alzeta mechanism	$T_{in} = 350K$	$u_{in} = 0.2\frac{m}{s}$	PeleLM

Table 1: Initial conditions for reaction path analysis and sensitivity analysis

1. both mechanisms well represent the flame structure (i.e., temperature and therefore heat release), as shown in Figure 2

2. both mechanisms provide good match for the H radical, which is a key species since it links methane and fluorine chemistry; however, there is a $\sim 20\%$ over-estimation of F and HF in the reduced model, as represented in Figure 3

3. compared to the Alzeta mechanism, the reduced mechanism does not capture in detail the conversion from CF_4 to HF, as shown in Figure 4 and 5 (in both Figures, the branching ratios shown are normalized to the integrated conversion in the reactor from CF_4 to CF_3)

4. using the Alzeta mechanism, a base mesh with spatial resolution $dx = 0.0016m$ and temporal resolution $dt \leq 1e-5s$ is required in order to accurately capture the flame topology.

5 Results and discussion

Given the limited duration of this study, combined with the difficulties encountered early in the investigation, the "results" we present consist primarily of demonstration calculations, and a single subsequent iteration with ALZETA to hone in on interesting aspects of parameter space. These results are followed by a collection of what we believe to be the primary "non-technical" findings of the study to be considered as the work moves forward.

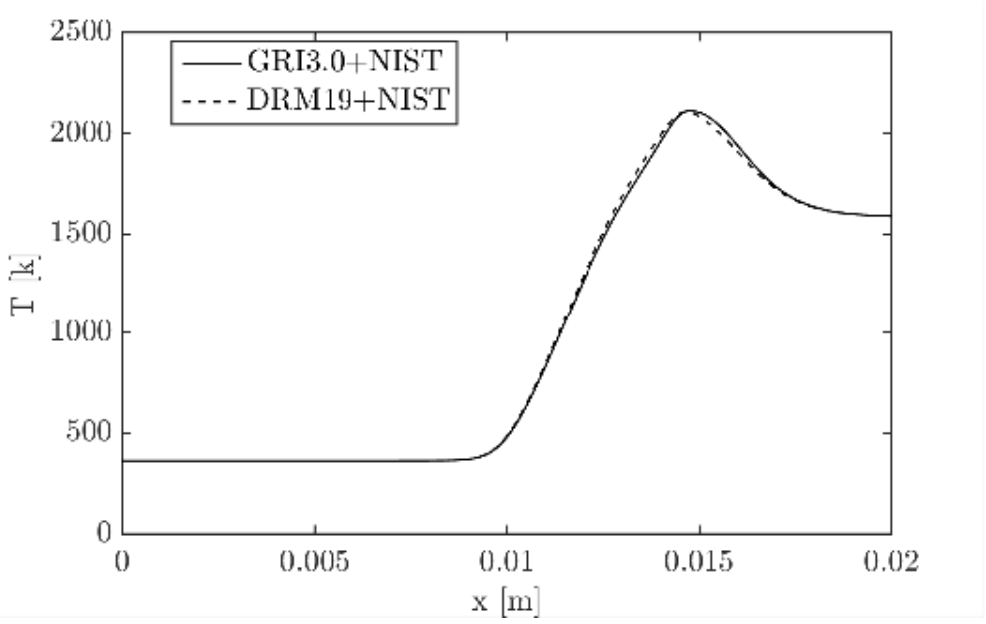

Figure 2: Comparison of temperature profile given by Alzeta (continuous line) and reduced mechanism (dash line) for 1D counterflow diffusion flame

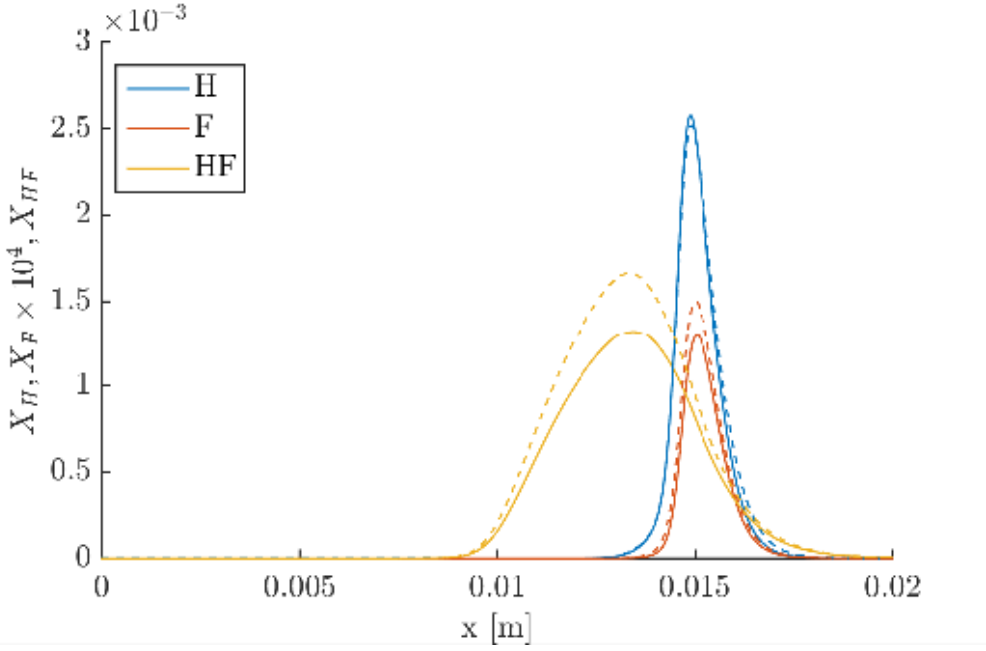

Figure 3: Comparison of some key species profiles given by Alzeta (continuous line) and reduced mechanism (dash line)

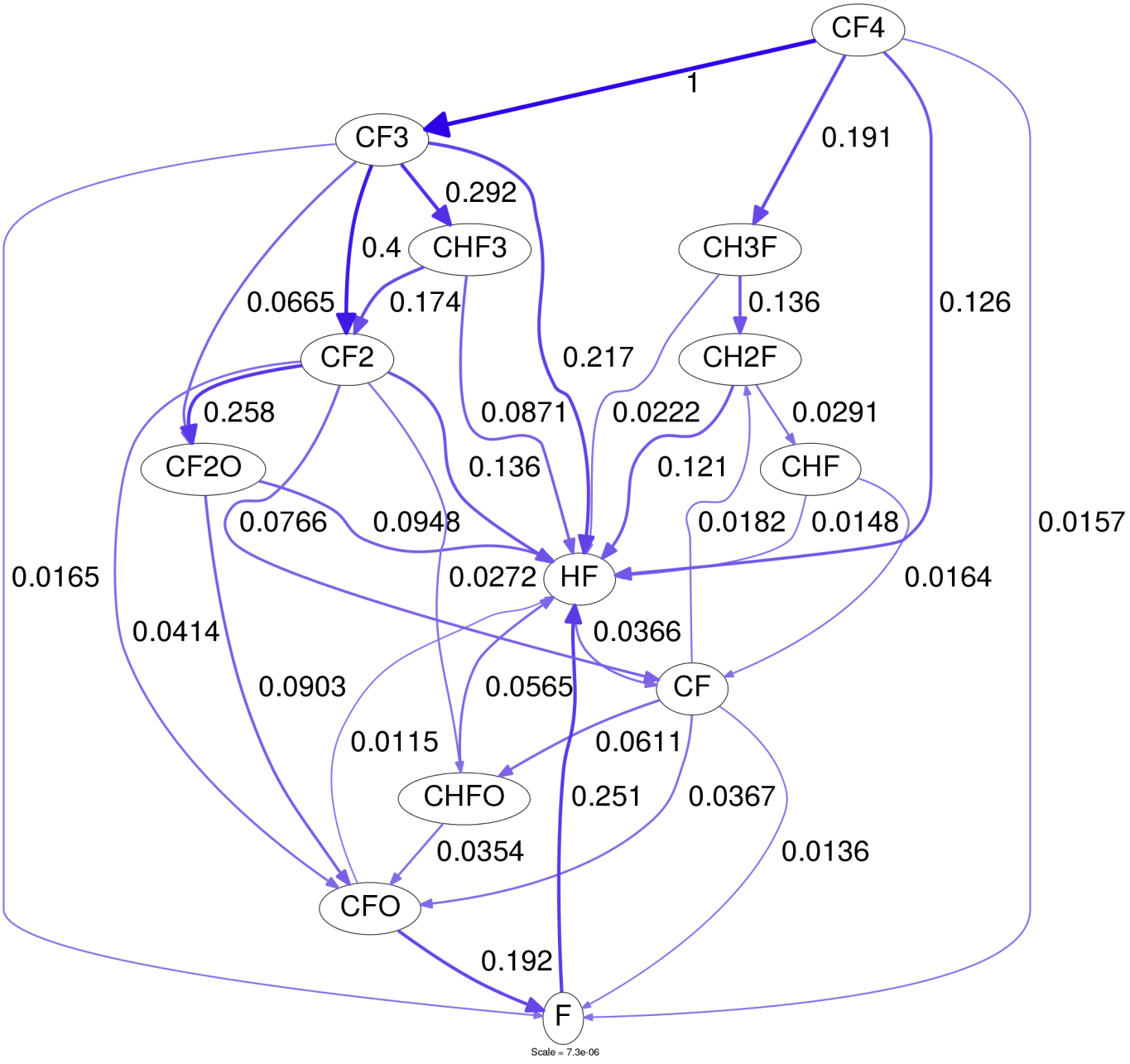

Figure 4: Reaction path diagram for Alzeta mechanism

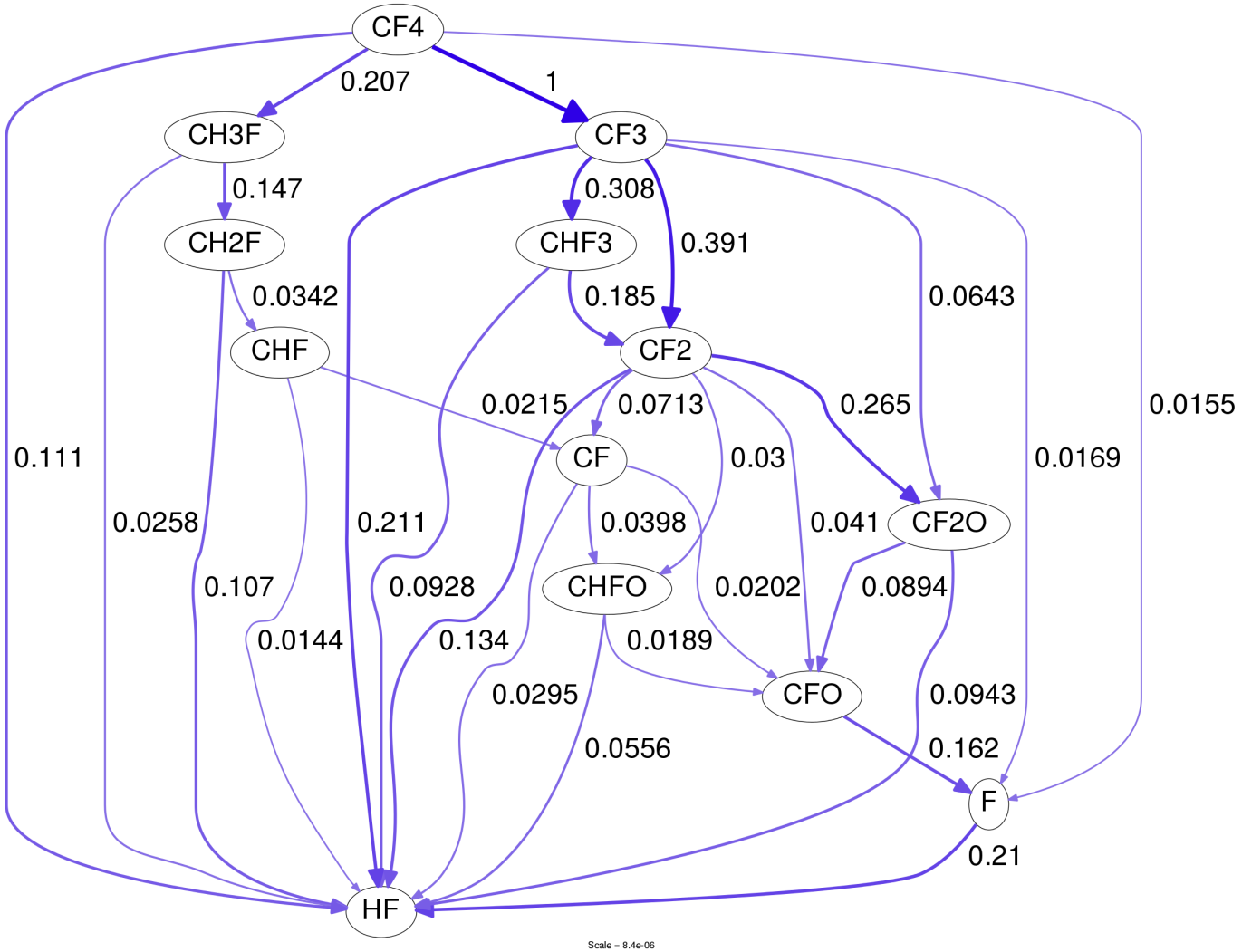

Figure 5: Reaction path diagram for reduced mechanism

5.1 Solution profiles and discussion

This section describes results obtained from two different sets of Case Studies:

- the first set includes 15 simulations and a single reactor configuration, as shown in Table 2 and Table 3
- the second set includes 10 simulations and three different reactor configurations, as shown in Table 4

Results have been obtained using a 2D axial-symmetric model of the Alzeta reactor, as shown in Figures 1; depending on the reactor configuration, a mixture of CH_4, O_2, N_2 and CF_4 is injected from the top face of the cylinder in different ways, as shown in Figure 1c, 1d and 1e. The constant flow rates of N_2 and CF_4 are identical for all the Case Studies, while those of CH_4 and O_2 are adjusted for each case, as shown in Table 3 and Table 4. In the laboratory device, a premixed flame is maintained around the porous inside walls of the lateral surface of the reactor, and its combustion products are used to heat the process stream gases; the design parameters for the premixed flame are the flow rate of main burner methane and the equivalence ratio, as shown in Table 3 and Table 4. The water-cooled walls below the porous burner surfaces are maintained at a constant temperature of 70°F via water cooling. Note that all inlet flow rates are considered to be steady over time; time-dependence arising from initial transients at device startup are ignored, since the device is designed for longer-time steady-state operation.

Results have been obtained using a single level grid of 256×3328 uniformly-sized cells. All simulations were carried out on the "Theta" supercomputer at the Argonne Leadership Computing Facility; each case ran on 8 compute nodes of Theta (each contains 64 cores), for a total of 512 cores. Since the main goal of this project is to minimize production of CF_4 by converting it into HF, we defined the steady state regime in terms of the integrated production rate of HF: when this quantity reaches a constant value over time, the system is considered steady, from the point of view of CF_4 consumption. We acknowledge that additional time is required for the product gases to move through and exit the bottom of the device. However, we observed that in the cases we considered, once the primary reaction zone was established, the subsequent flows and device residence times downstream had little impact on chemical conversion process. With this definition, the wall-clock time required to reach "steady state" with PeleLM was approximately 7-10 days for each case, and the total amount of CPU time required was:

- Approximately 2M CPU hours (total) for the first set of Case Studies
- Approximately 1.5M CPU hours (total) for the second set of Case Studies

5.2 Results for the 1st SET of Case Studies

This first set of runs was based on a single jet configuration: the process gases (e.g. CF_4+CH_4+air) are injected through the single jet located at the center of the top boundary of the reactor, as shown in Figure 1c. A list of the design parameters used for these simulations can be found in Table 2 and Table 3.

Figure 6 shows the time evolution of the integrated production rate of HF: since the flow rate of CF_4 is identical for all cases considered, it is not surprising that most of the simulations stabilize around the same value. However, several cases exhibited profiles such as that shown for Case 15. This behavior results from the fact that the CF_4 consumption was too slow in these cases and the exit stream at the reactor bottom contained a significant fraction of unreacted CF_4. Also, many of the cases exhibit a transitory peak in integrated HF production early in the evolution, as a result of transients due to startup - a large vortical structure is generated at the process stream inlet and propagates downward through the reactor.

These results suggest that, depending on how the fluorine chemistry evolves in the combustion zone, the flame structure can be of two different types:

a) The CF_4 reacts completely in the flame zone. Here the flame assumes a downward-pointed conical shape; CF_4 is converted to HF, which then advects downstream and out of the reactor domain

b) The CF_4 reactions are slow, in which case much of the CF_4 exits the bottom of the domain unreacted. Certainly, this is a condition we want to avoid.

The following figures show the time evolution of some of the most relevant data fields; plots have been obtained using the open-source visualization package "yt" [8]. For sake of simplicity, we do not report results for all the Case Studies involved in this first set of runs; instead, we simply show a comparison between a case in which all CF_4 reacts in the flame zone and a case in which unreacted CF_4 advects out of the reactor.

In particular [1]:

- Figures 7 to 12 refer to Case 11
- Figures 13 to 18 refer to Case 15

[1]Notice: the units of both radial and velocity profile should be m/s, and not cm/s.

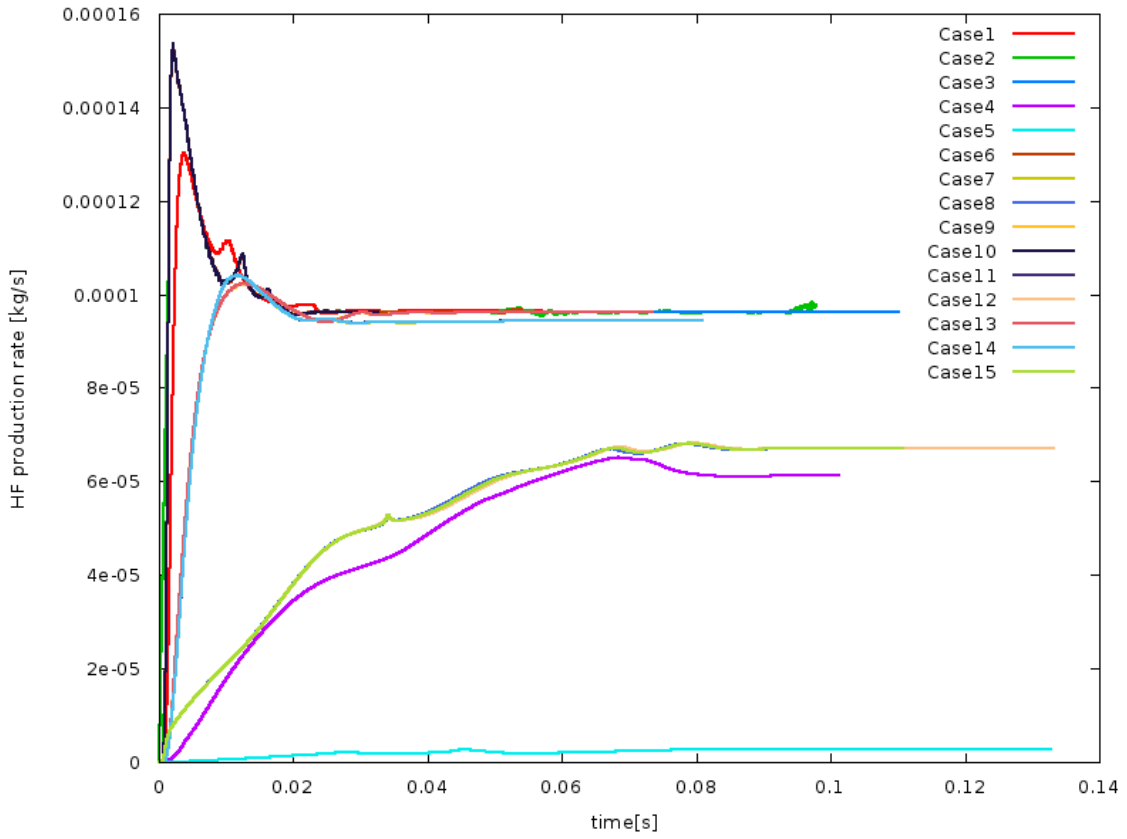

Figure 6: Time evolution of the integrated production rate of HF for the 1^{st} SET of Case studies

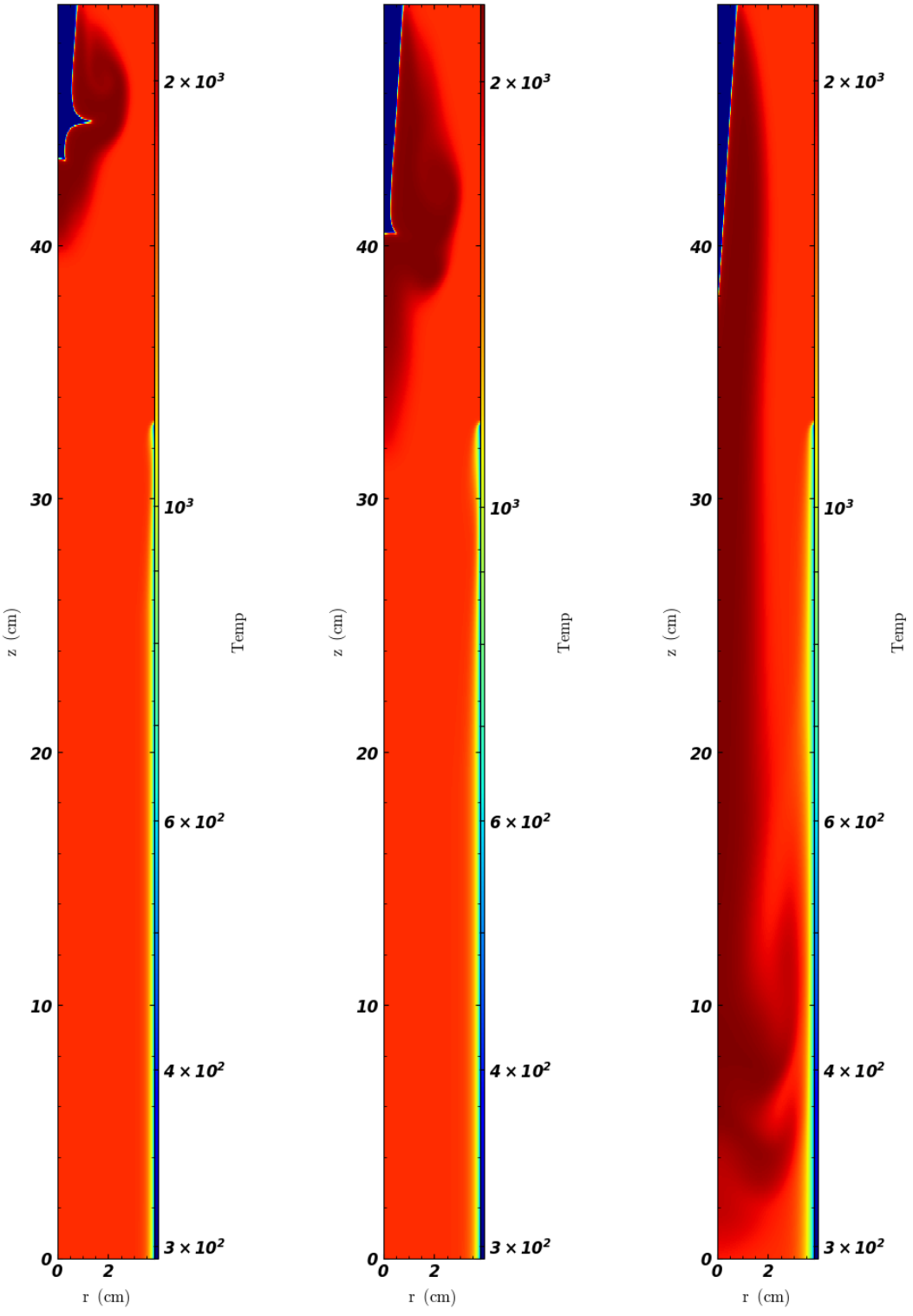

Figure 7: Case 11 - Time evolution of temperature profile

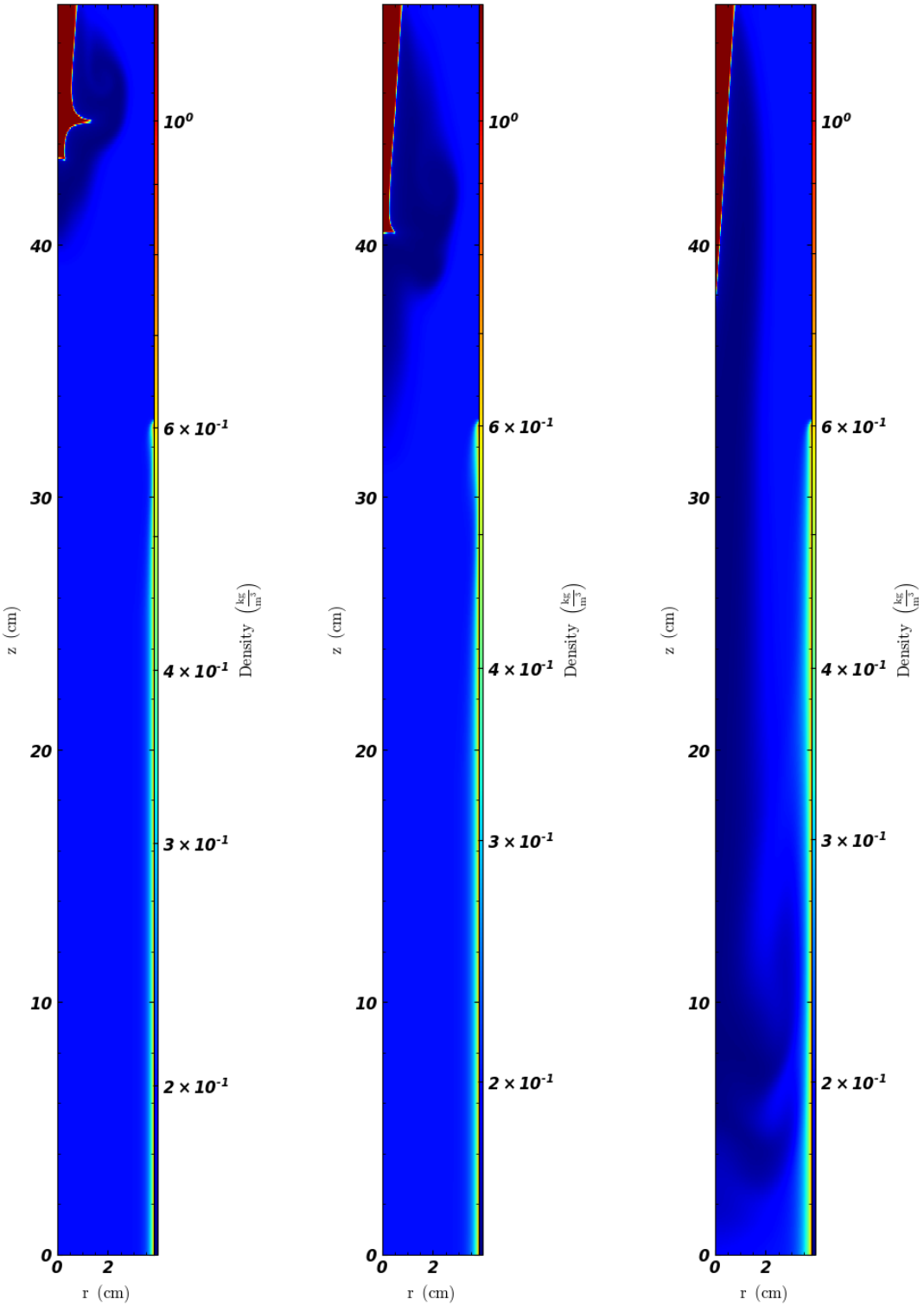

Figure 8: Case 11 - Time evolution of density profile

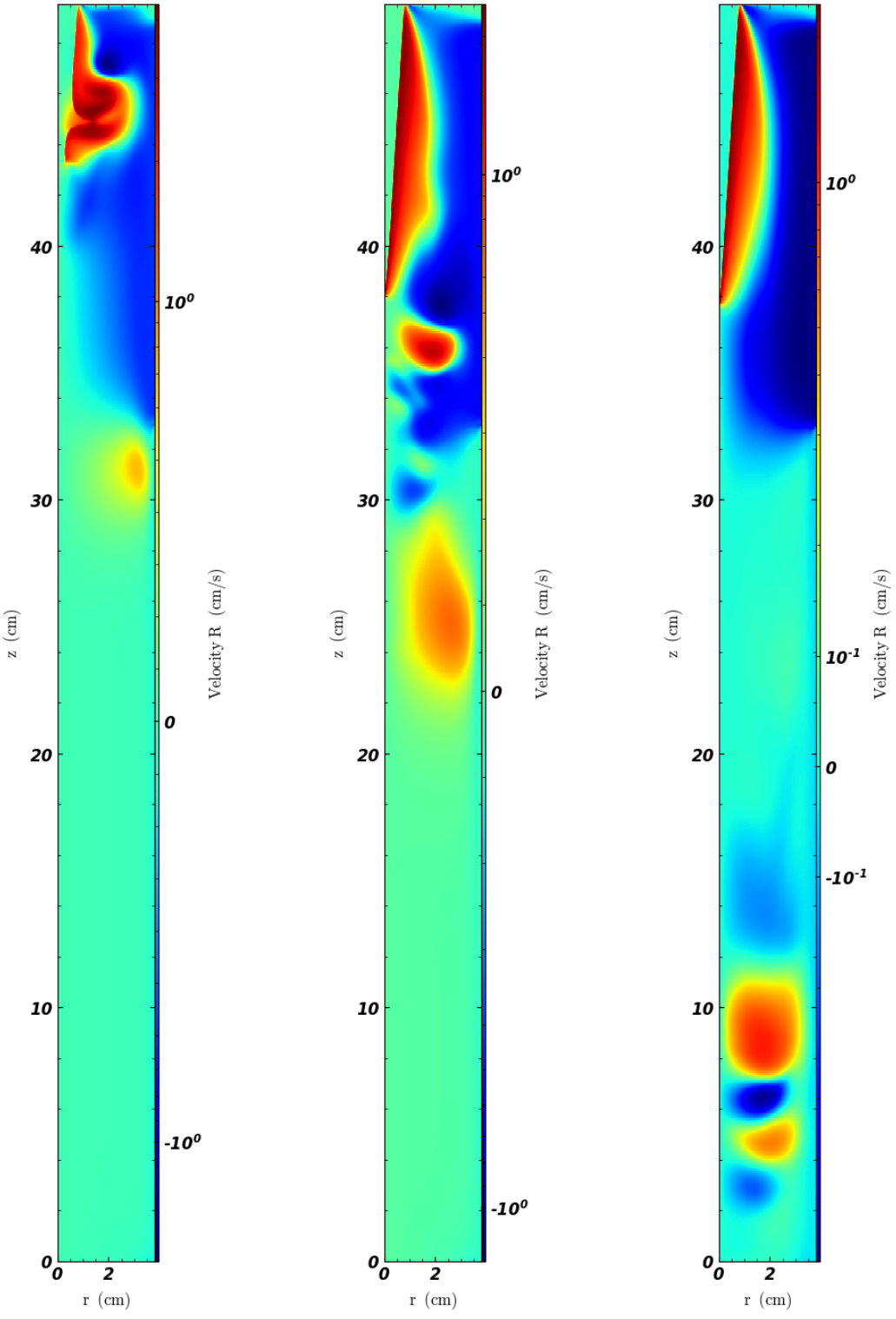

Figure 9: Case 11 - Time evolution of radial velocity profile

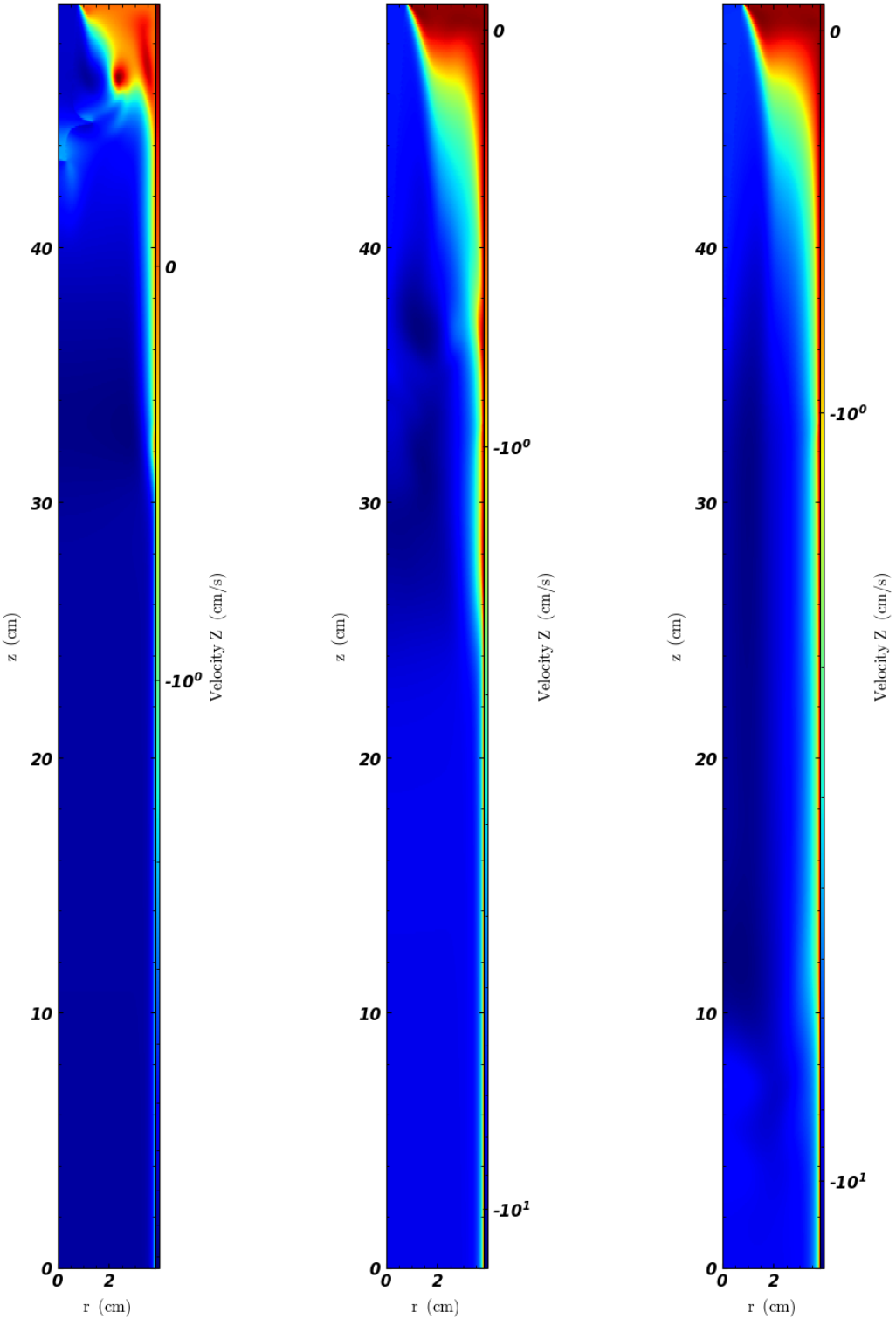

Figure 10: Case 11 - Time evolution of axial velocity profile

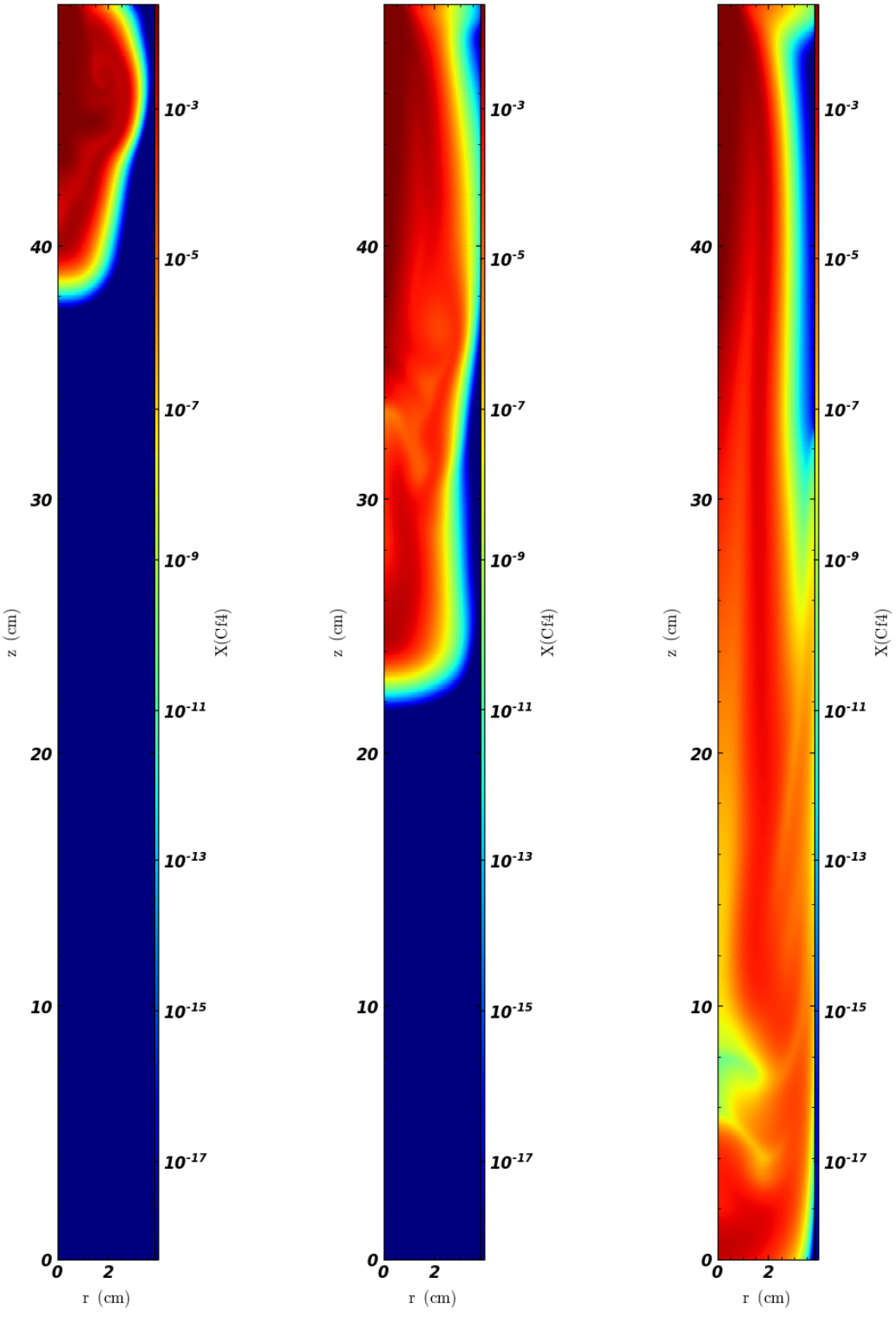

Figure 11: Case 11 - Time evolution of CF_4 molar fraction profile

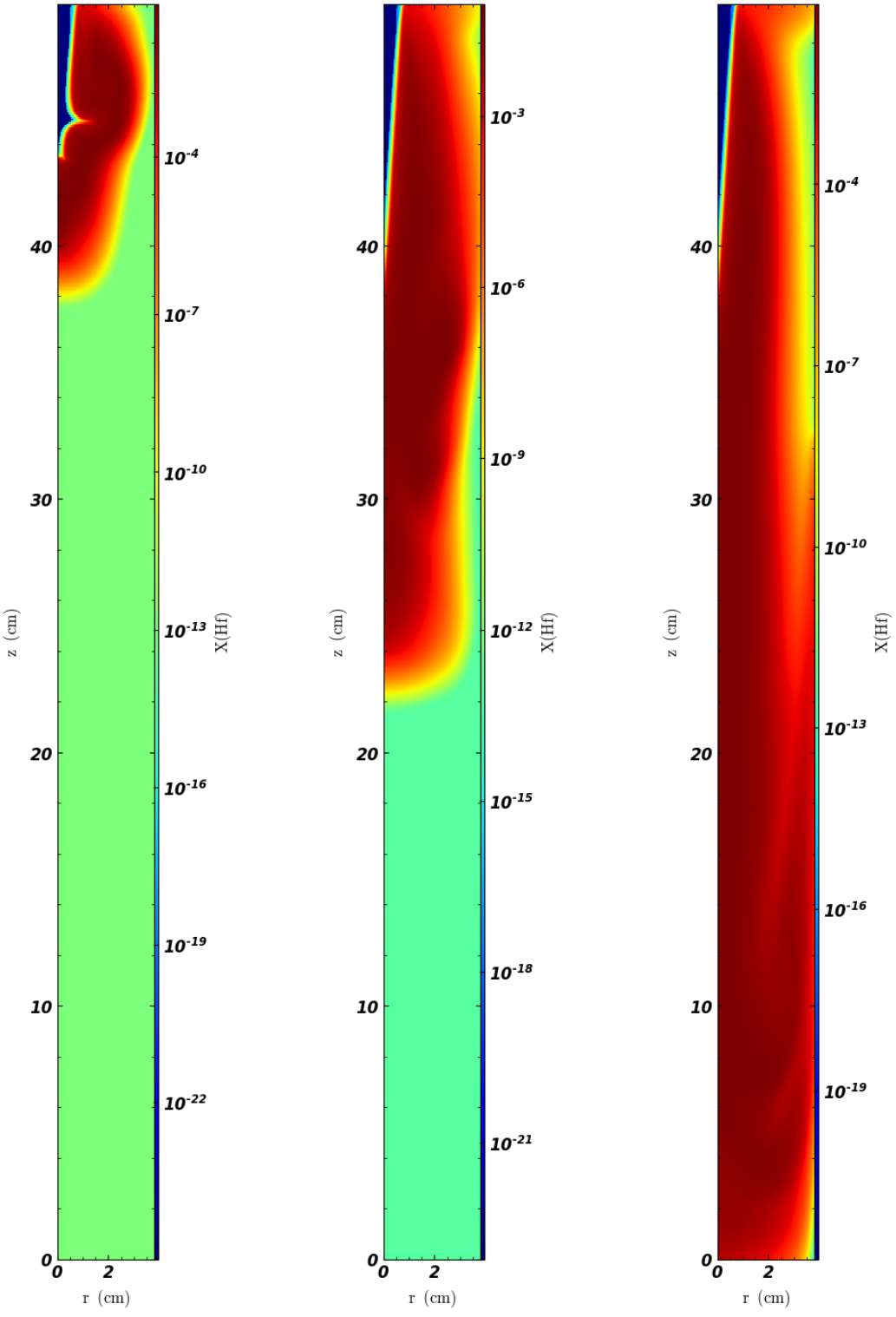

Figure 12: Case 11 - Time evolution of HF molar fraction profile

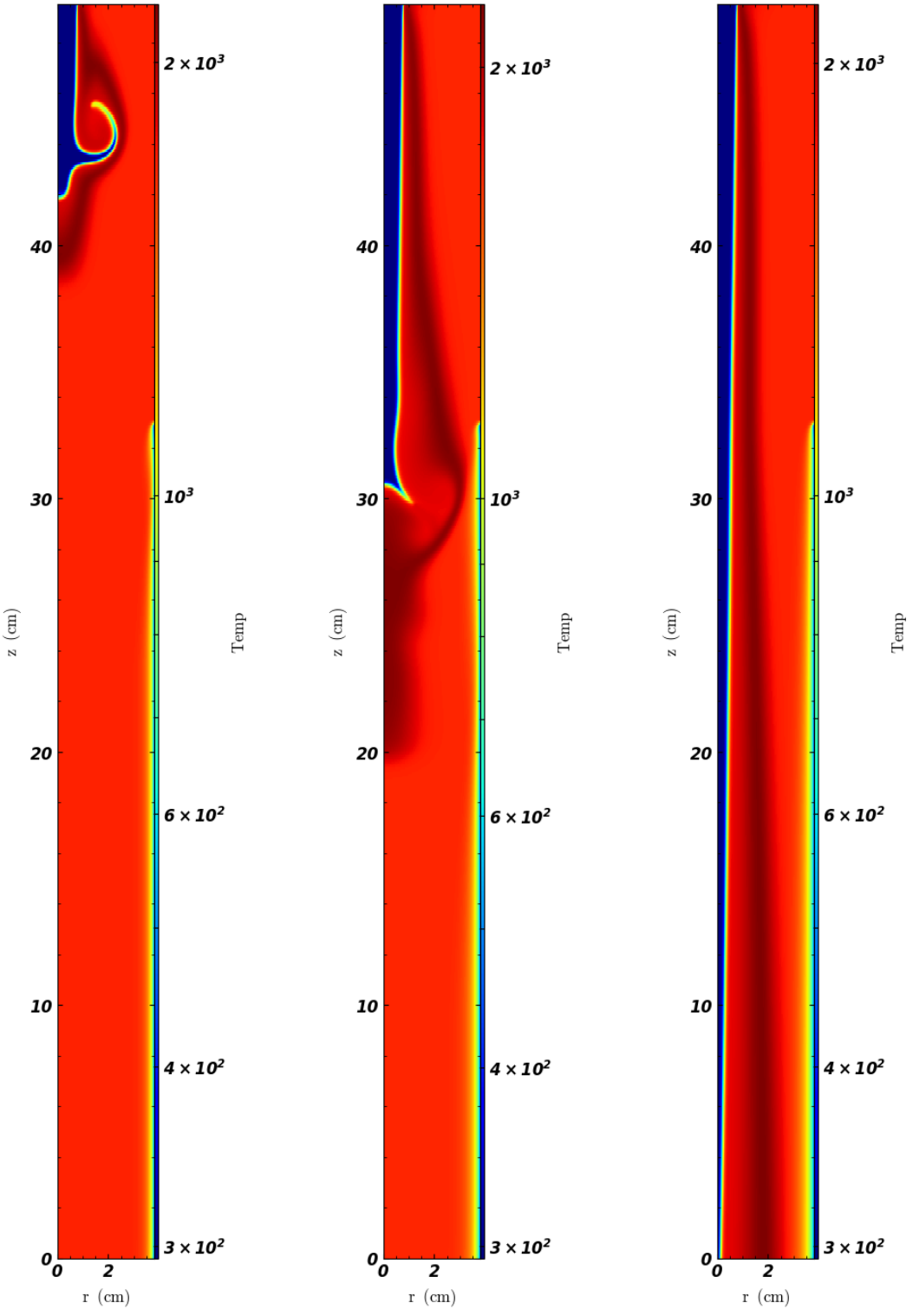

Figure 13: Case 15 - Time evolution of temperature profile

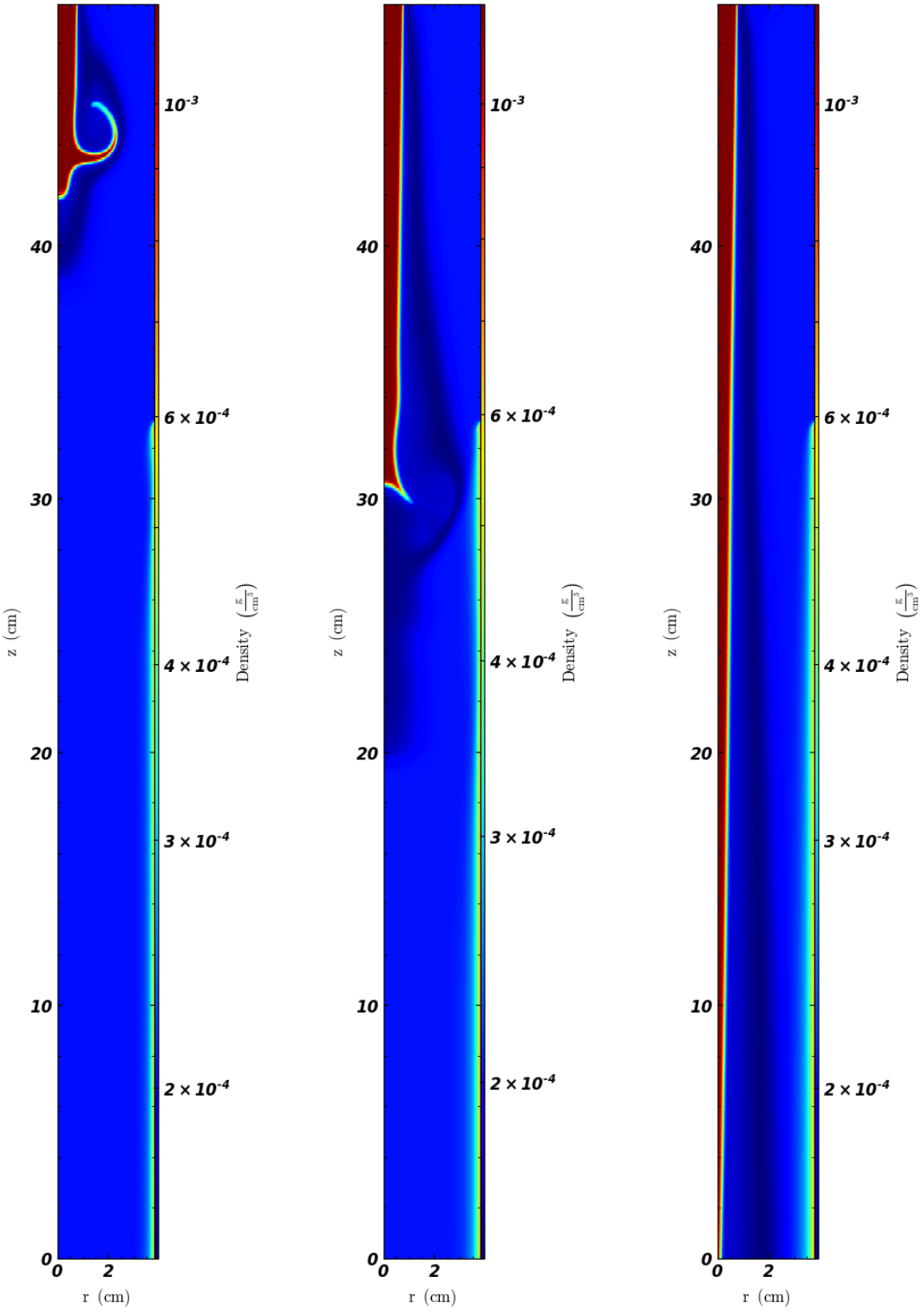

Figure 14: Case 15 - Time evolution of density profile

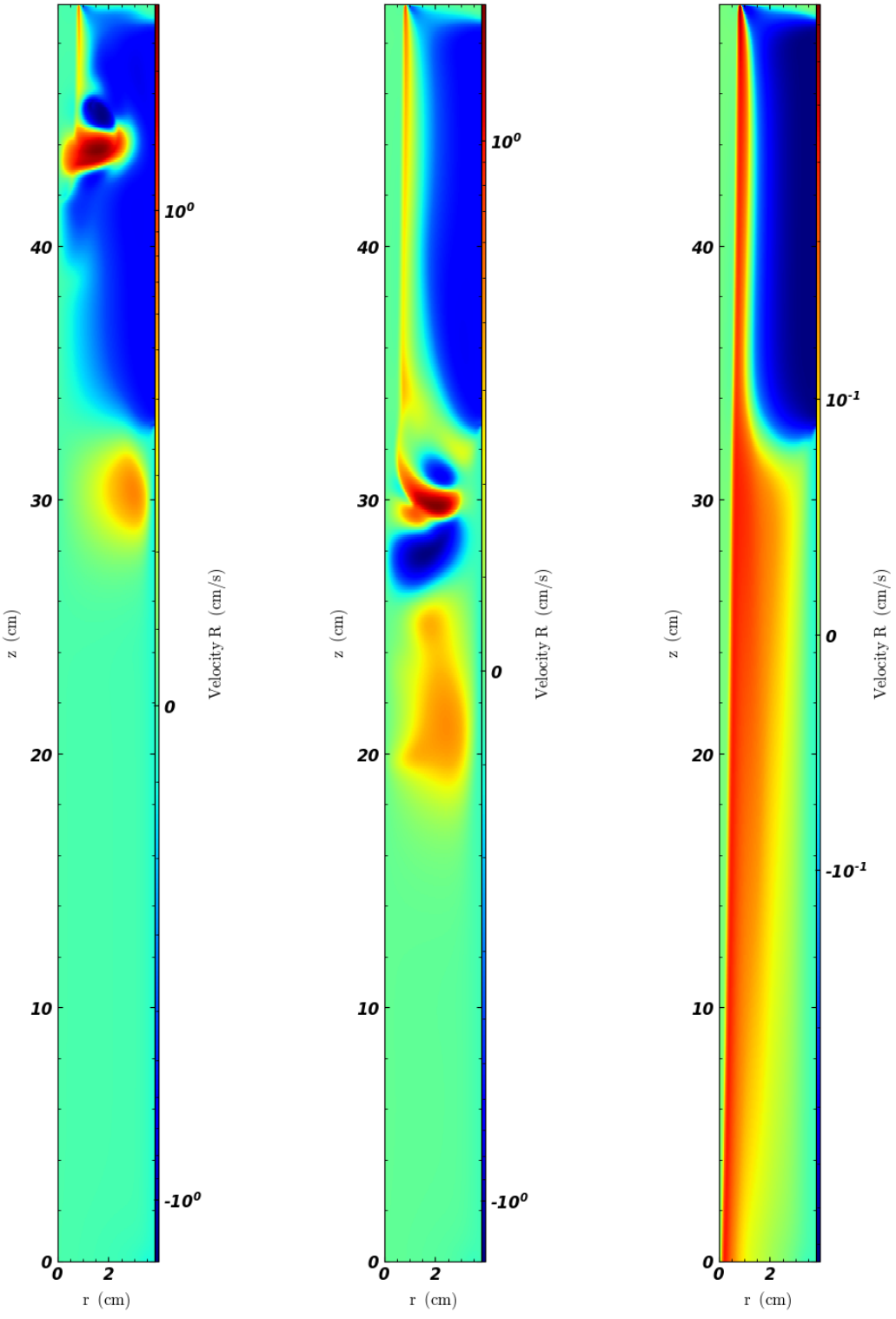

Figure 15: Case 15 - Time evolution of radial velocity profile

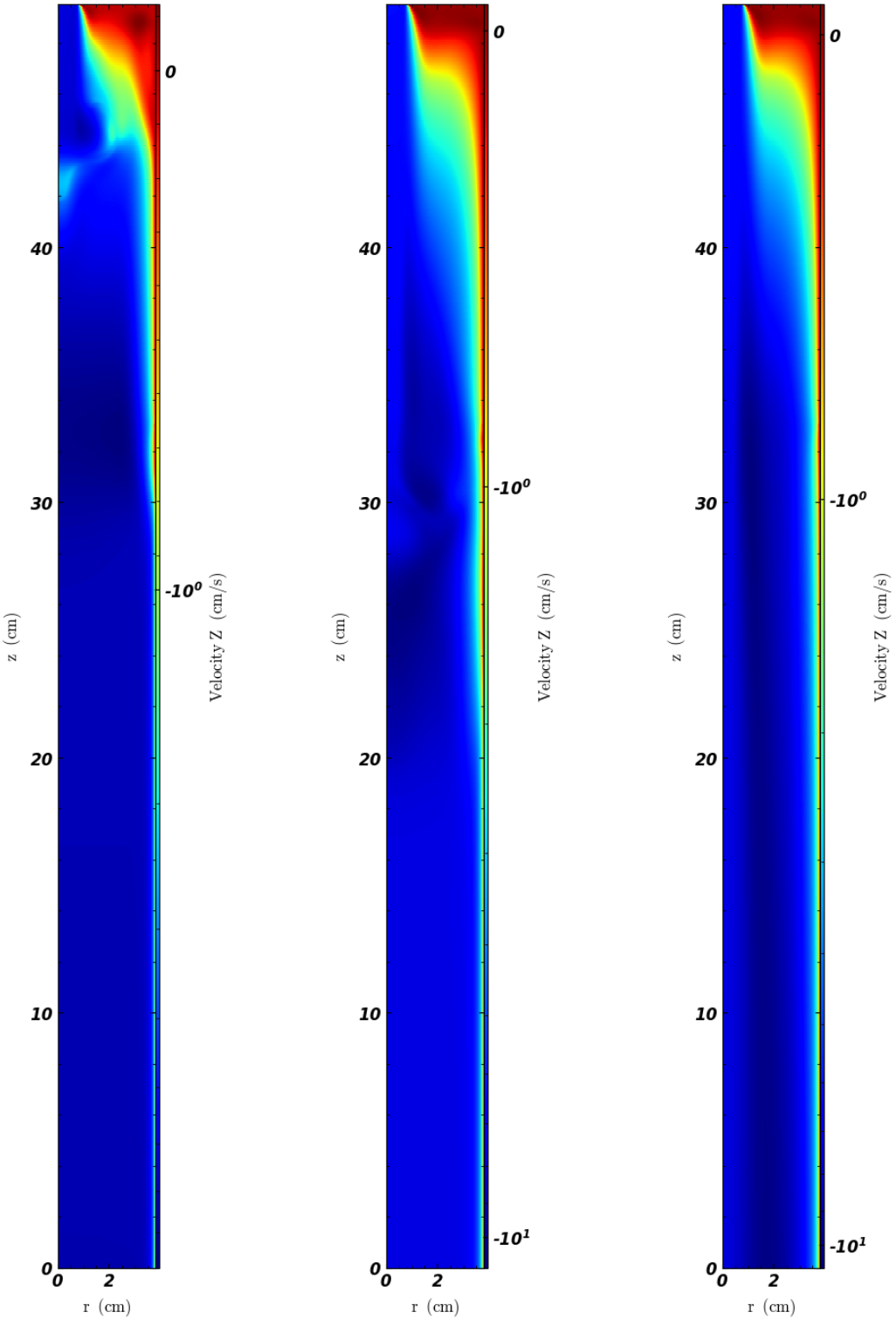

Figure 16: Case 15 - Time evolution of axial velocity profile

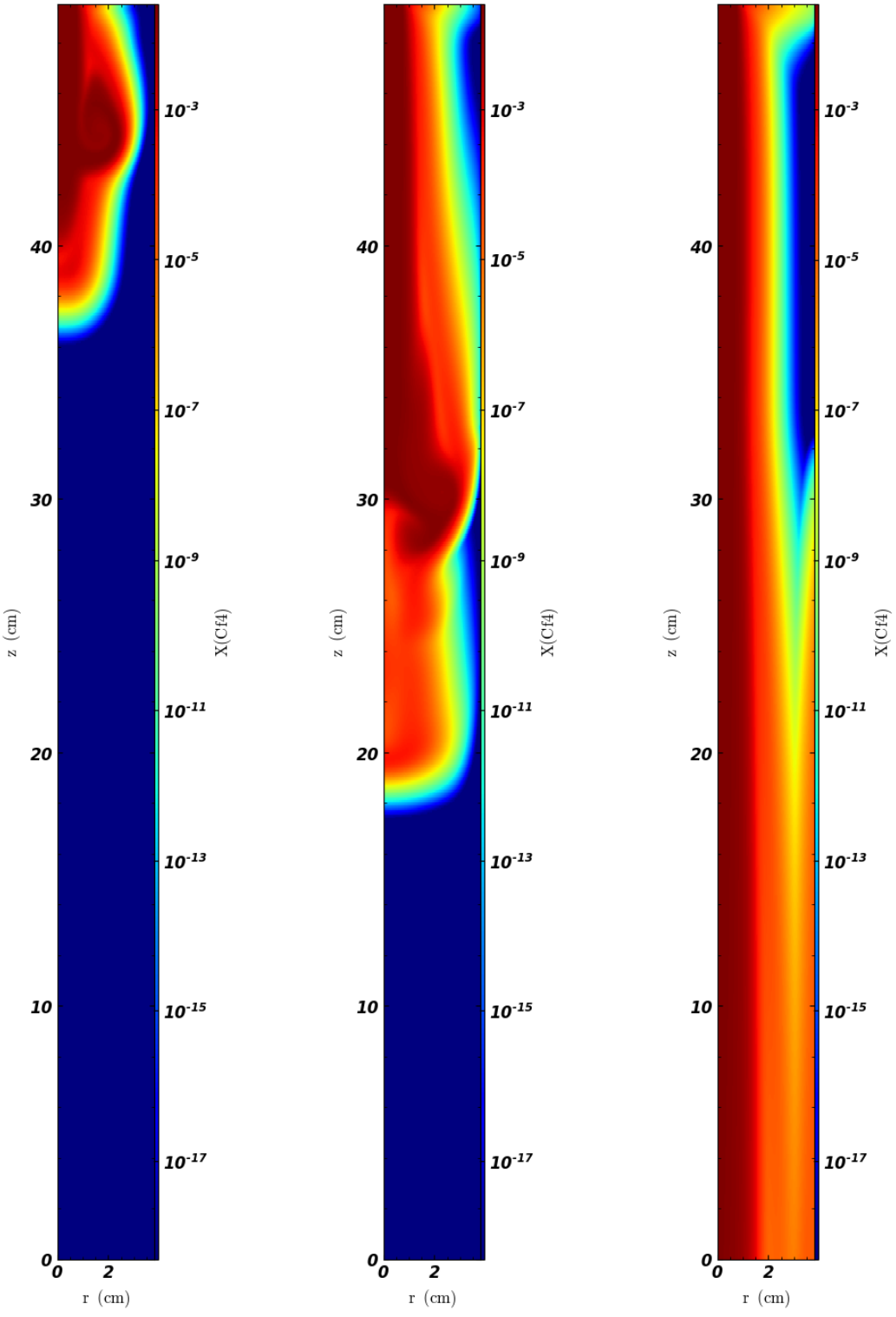

Figure 17: Case 15 - Time evolution of CF_4 molar fraction profile

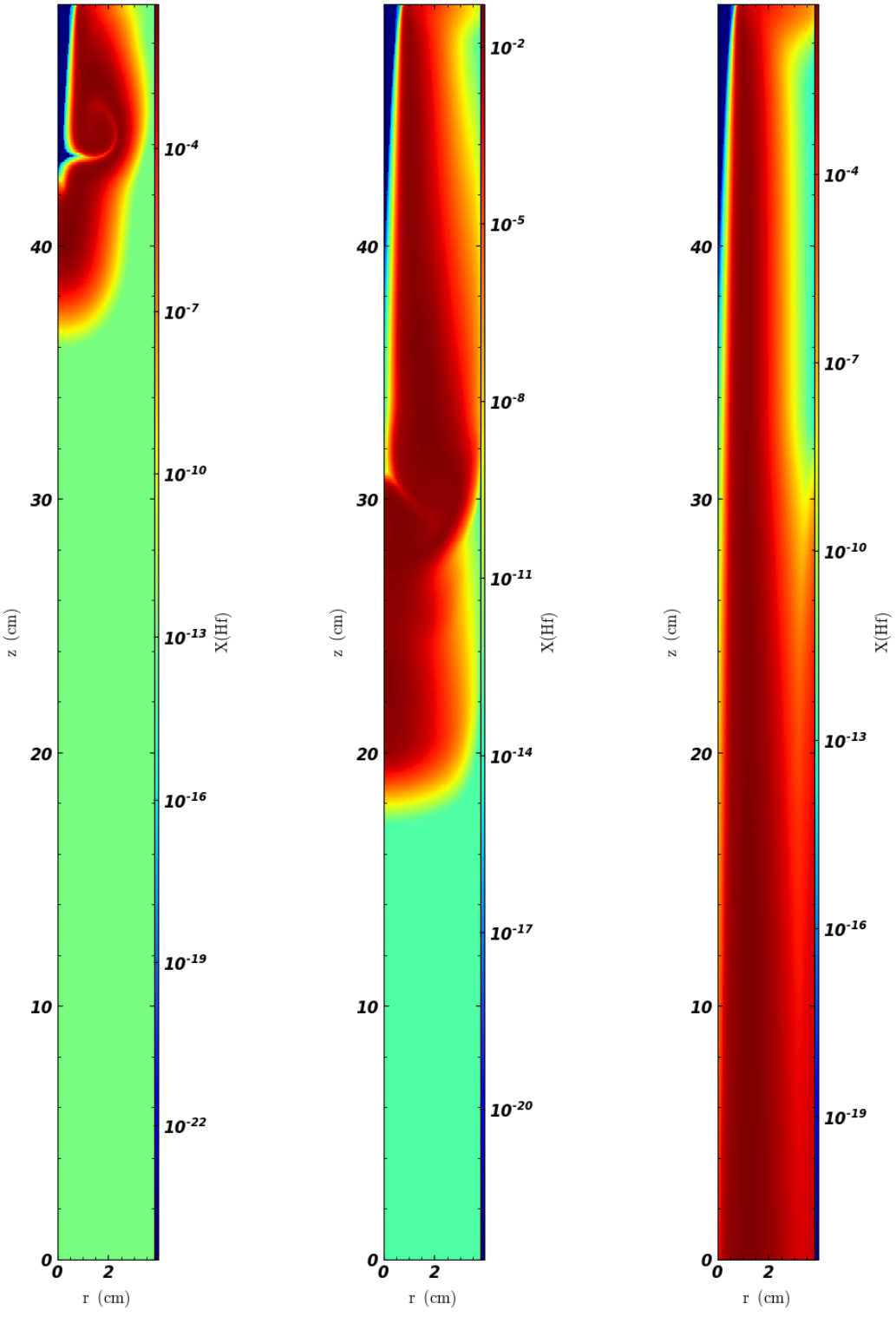

Figure 18: Case 15 - Time evolution of HF molar fraction profile

5.3 Results for the 2nd SET of Case Studies

Upon initial review of the early results, the researchers at ALZETA created a second set of cases to study:

- Additional single jet cases (Case 1, Case 2, Case3): as in Set 1, process gases are injected at the center of the top boundary, as shown in Figure 1c
- Concentric nozzle cases (Case 4, Case 5, Case 6, Case 7): process gases are injected through the inner nozzle, while CH_4 is fed through the annulus, as shown in Figure 1d
- Single jet, and a porous top wall (Case 8, Case 9, Case 10): process gases are injected through the single jet, while air or CH_4 is fed through a new top wall fabricated from a porous material, as shown in Figure 1e. [2]

A list of the design parameters used for these simulations can be found in Table 4.

Figure 19 shows the time evolution of the integrated HF for the 2^{nd} set of Case Studies; as for the 1^{st} set, since the initial flow rate of CF_4 injected in the system is the always the same, Cases with the same geometry stabilize around the same value. However, it is evident that the geometry of the process inlet strongly affects the flame behavior, and subsequently the time required to reach steady state. In fact, results for Case1, Case2 and Case3 are very similar those from the majority of the Case Studies of the 1^{st} SET: most of the CF_4 reacts in the flame zone to forms HF, which then advects downstream; the flame assumes the typical conical shape. Case4, Case5, Case6 and Case7 exhibit a slightly different behavior: the flow coming from the annulus induces strong vortical structures at the flame surface, which then propagates downstream until the vortex detaches; the flame tip retreats slightly upward until it finds a steady position. The physical time to reach teady solutions in the concentric nozzles configurations was nearly twice that as those with the single jet configuration. Differences in the initial dynamics notwithstanding, CF_4 typically reacts away completely in the flame zone leaving negligible amounts in the product stream.

The following figures show the time evolution of the most relevant data fields; again, for sake of simplicity we do not report results for all the Case Studies. Since Cases with the same geometry exhibit very similar behavior, we show only one Case per each reactor configuration. In particular:

- Figures 20 to 25 refer to Case 1 (single jet)

[2] Results for these three Case Studies have not been included in the current report since simulations have not reached steady state yet.

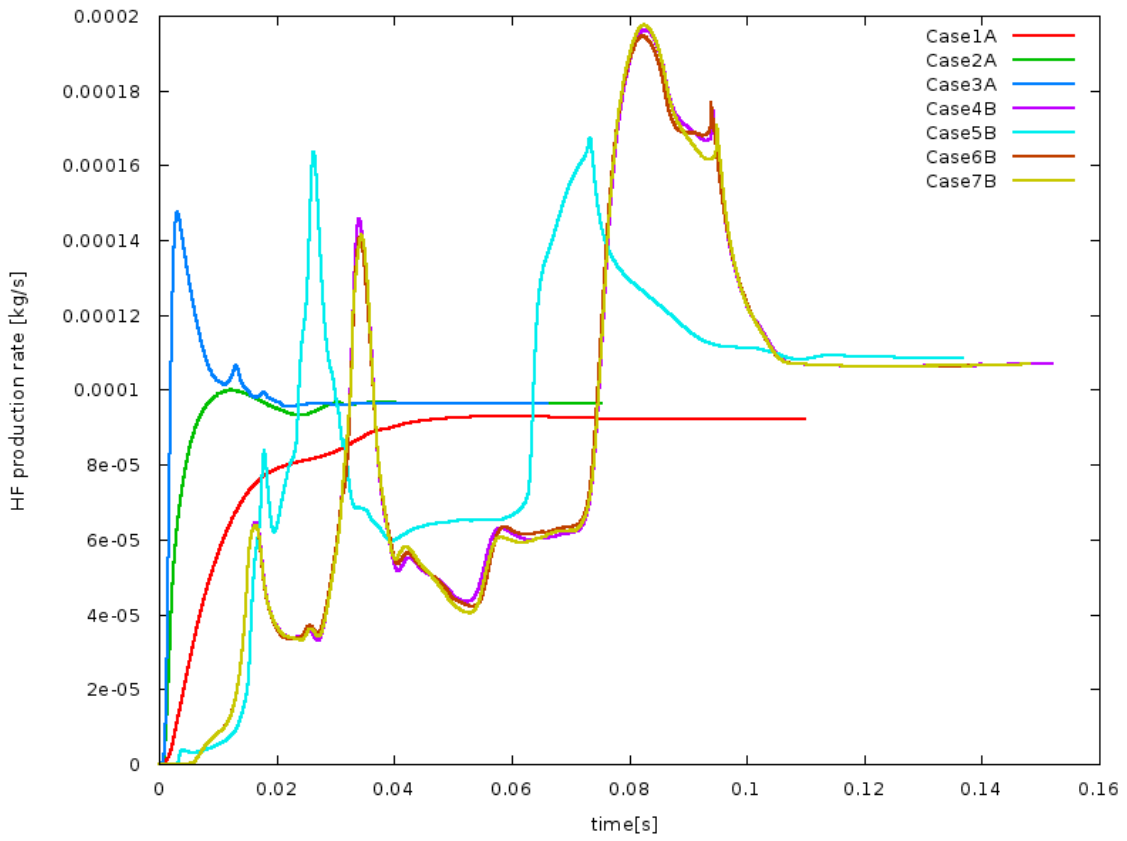

Figure 19: Time evolution of the integrated production rate of HF for 2^{nd} SET of Case studies (Case1 to Case7 only)

- Figures 26 to 31 refer to Case 4 (concentric nozzles)

Independent Variables							
Inject Flow	**Design**		**DOEx Levels**				
Methane Inject	10	slpm	20%	0	-20%	-40%	-60%
Oxygen Inject	18	slpm	20%	0	-20%	-40%	-60%
Main Burner							
Main Burner Methane	5.375	slpm	-25%	0	25%		
Equivalence Ratio	0.625	-		0.625	0.714		
Constants							
Process Flow							
Process Nitrogen	50	slpm					
Process CF4	2	slpm					
Isothermal Wall Temp	70	deg F					

Table 2: List of independent variables defined for the 1^{st} SET of Case Studies

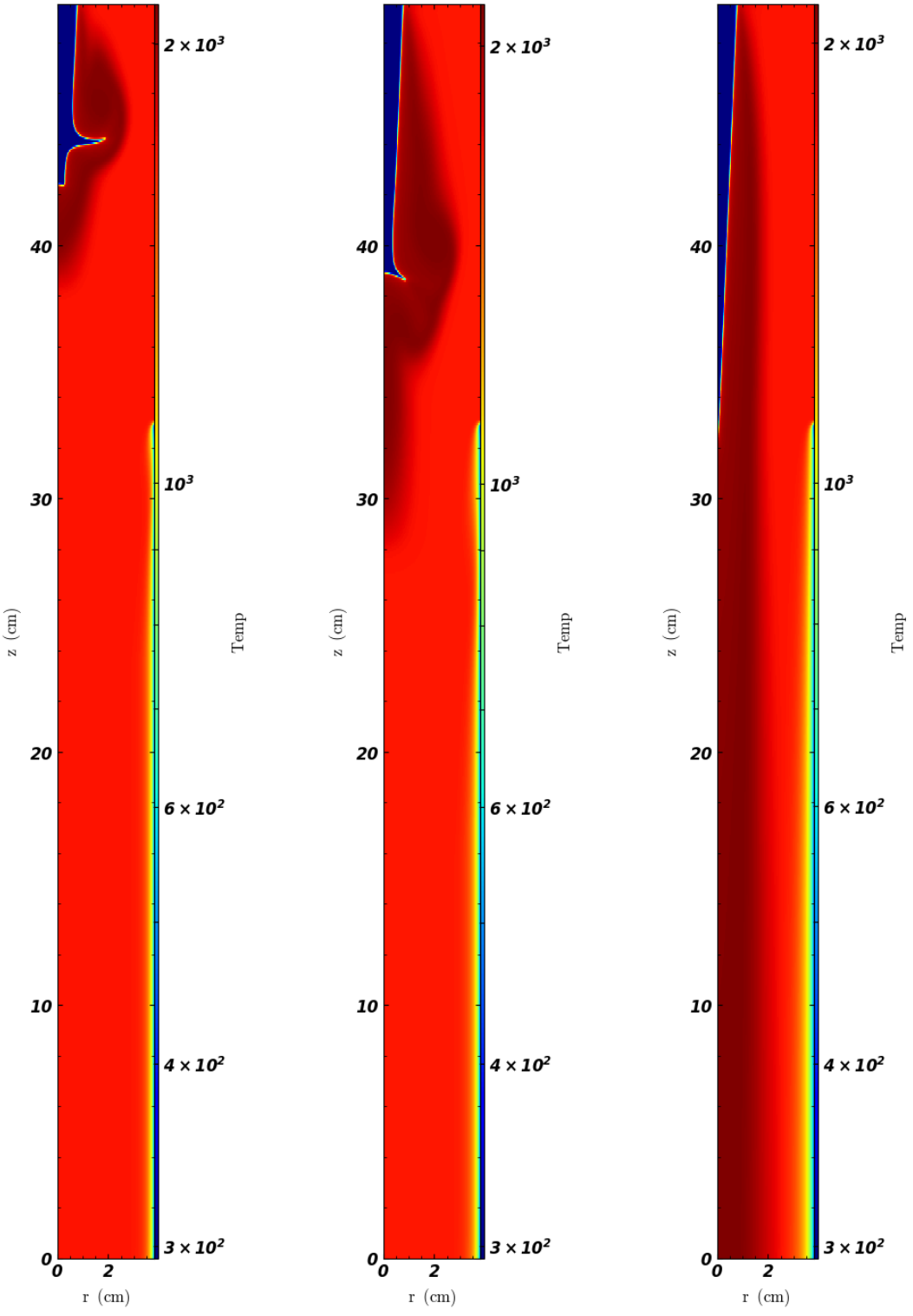

Figure 20: Case 1 - Time evolution of temperature profile

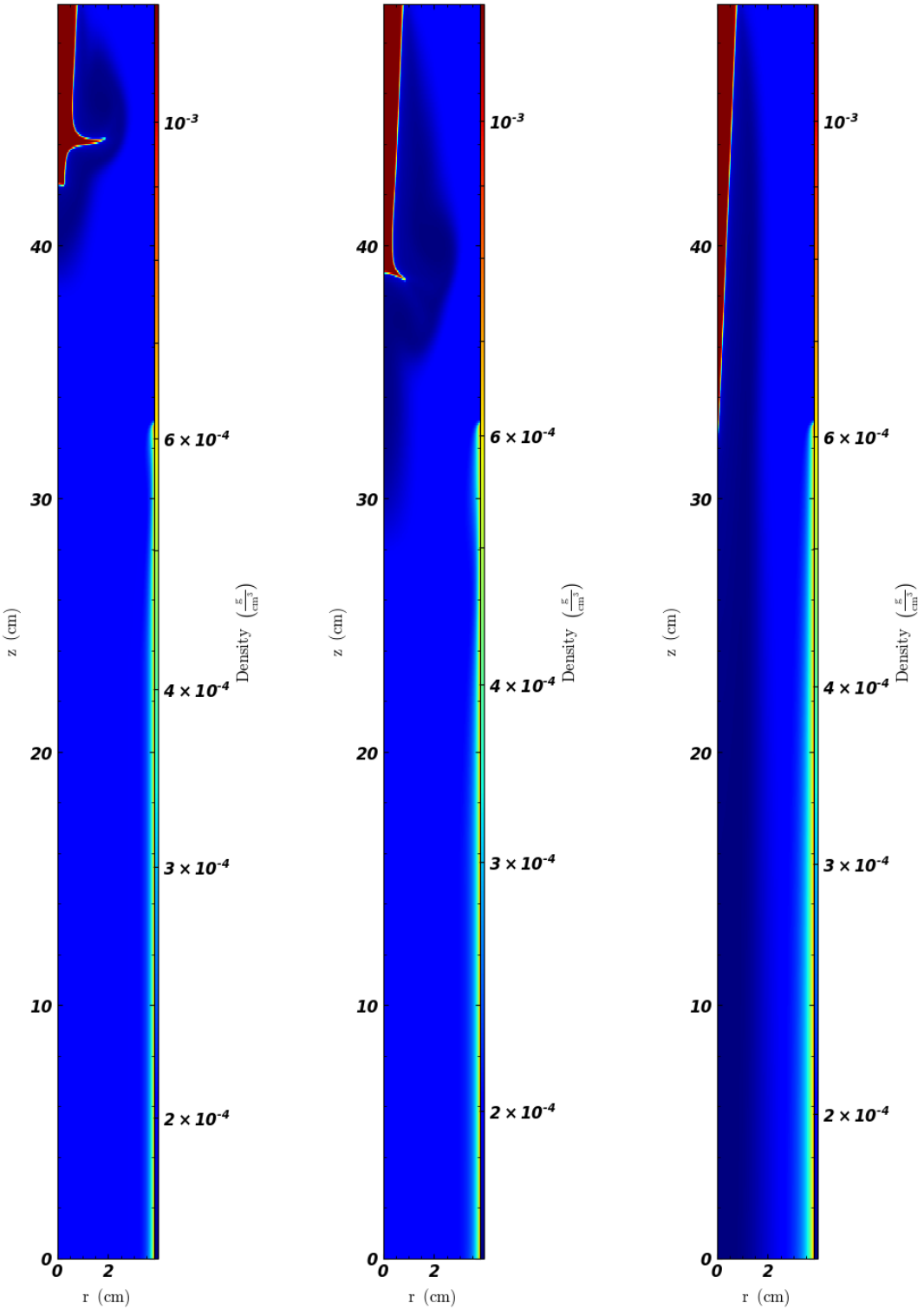

Figure 21: Case 1 - Time evolution of density profile

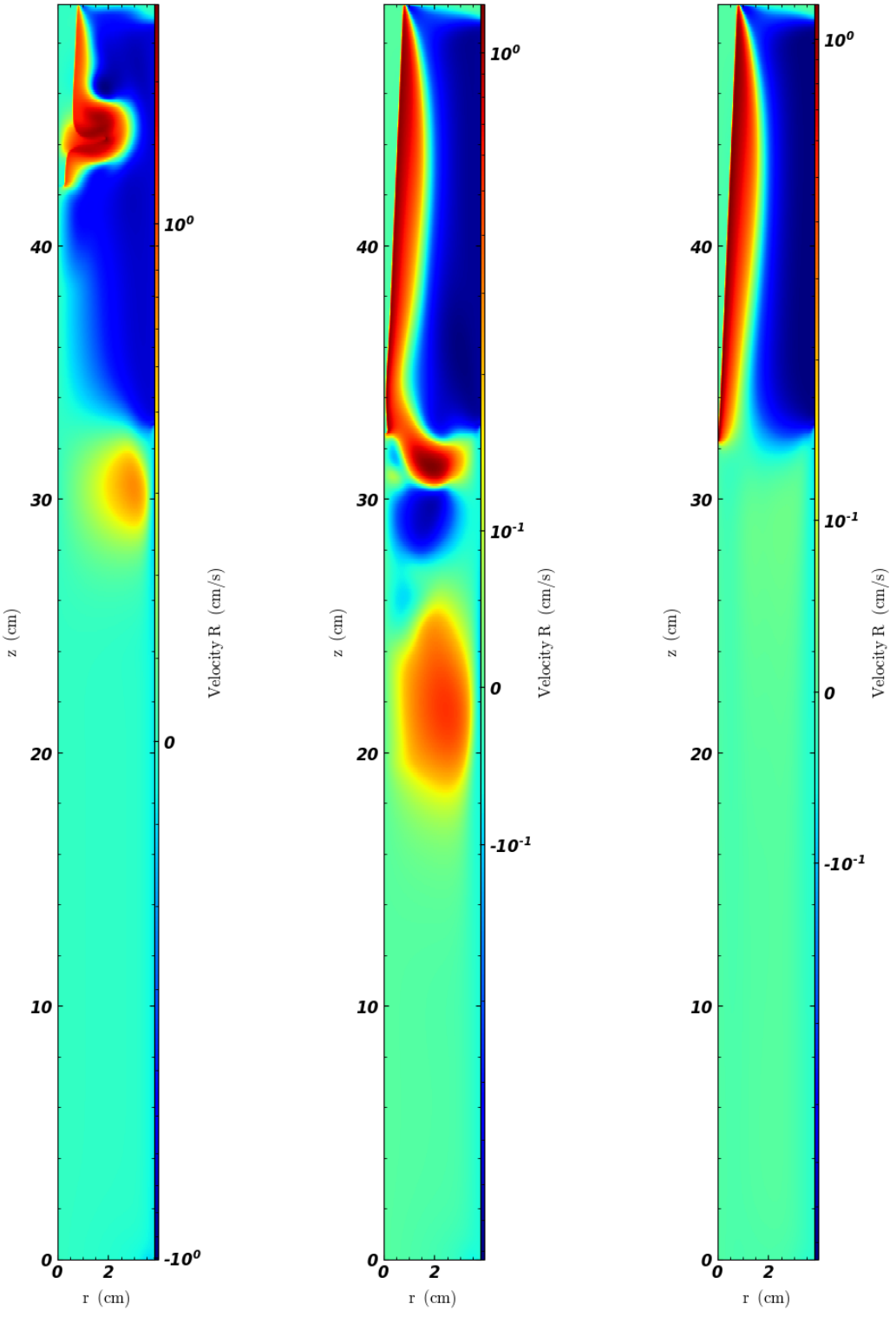

Figure 22: Case 1 - Time evolution of radial velocity profile

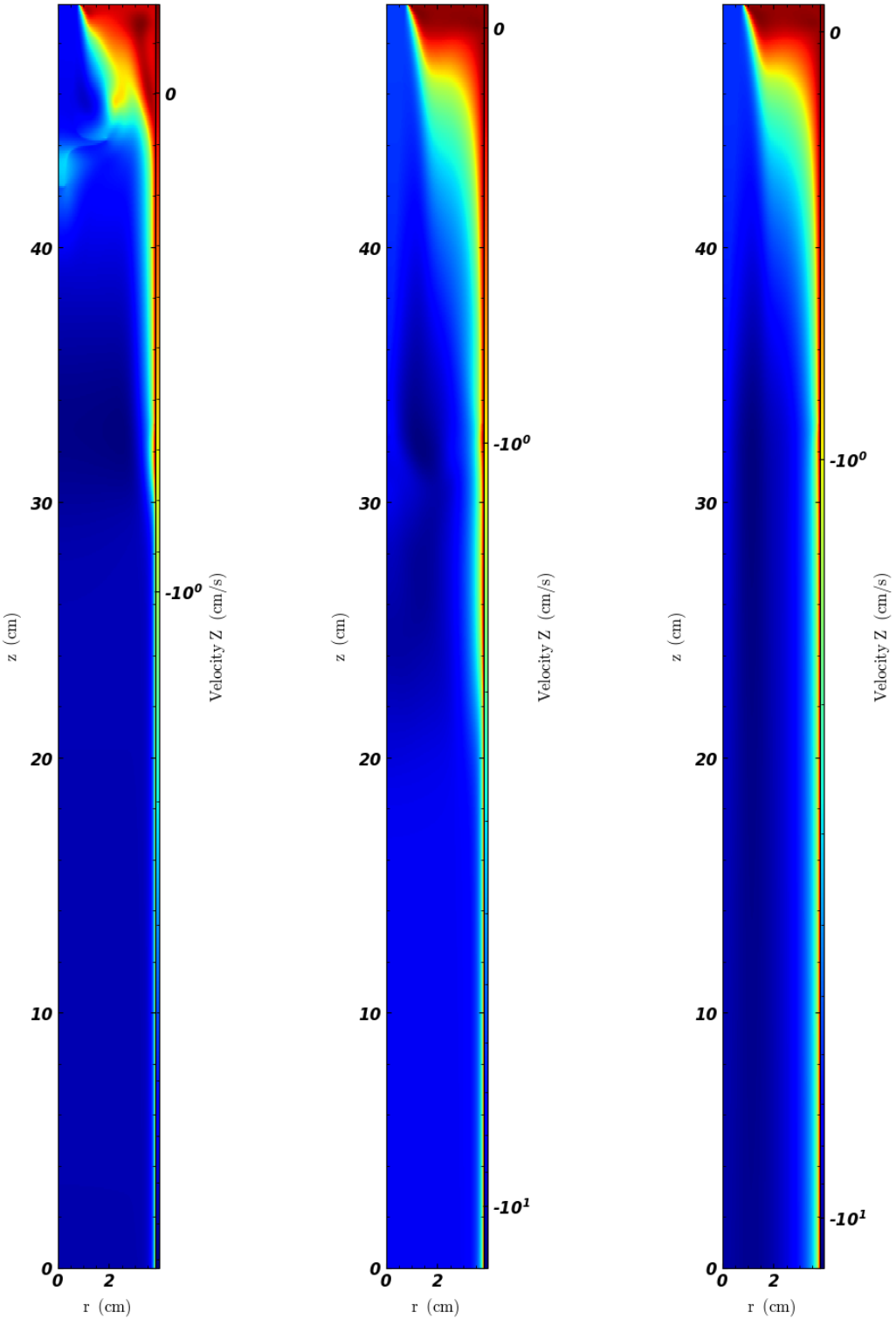

Figure 23: Case 1 - Time evolution of axial velocity profile

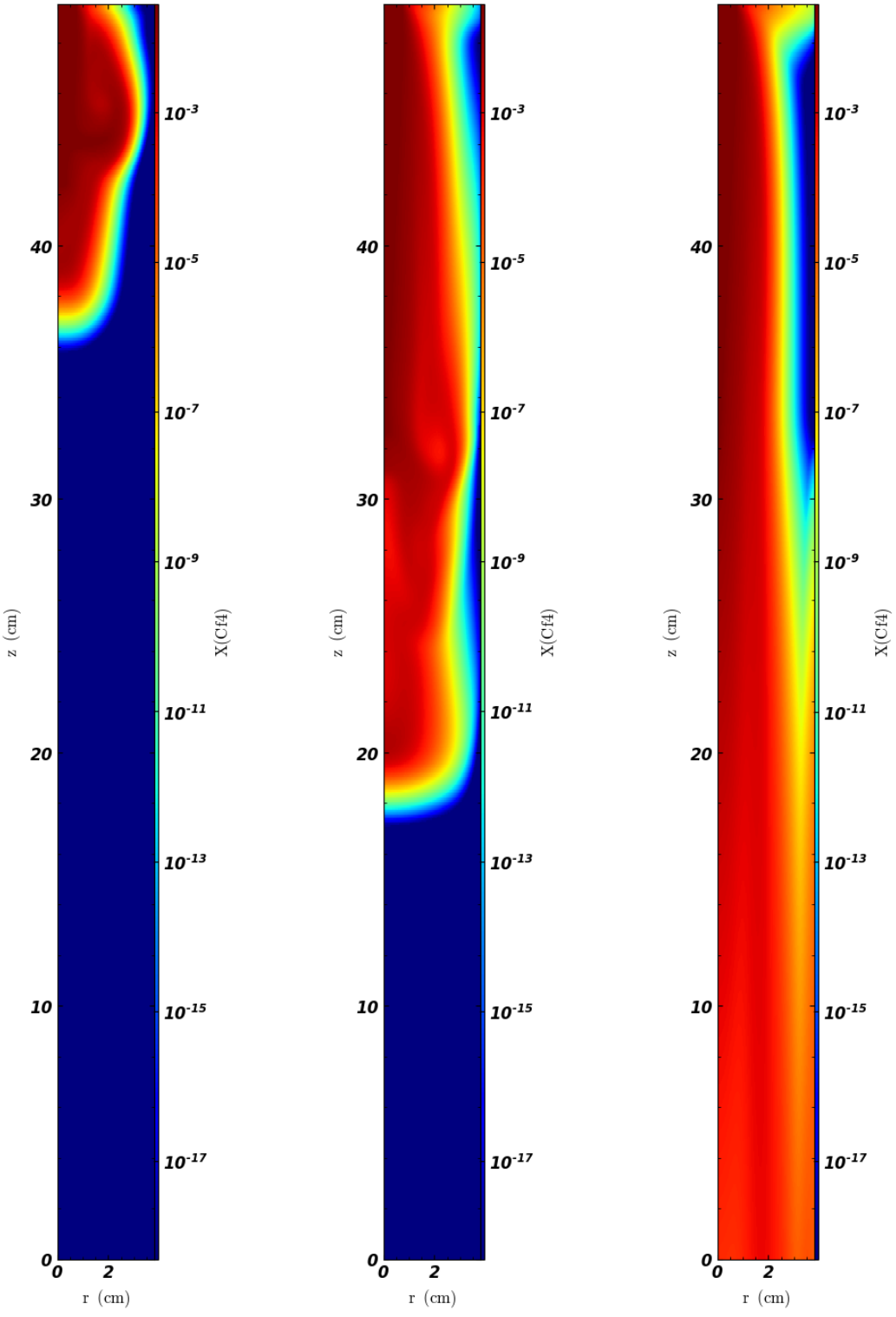

Figure 24: Case 1 - Time evolution of CF_4 molar fraction profile

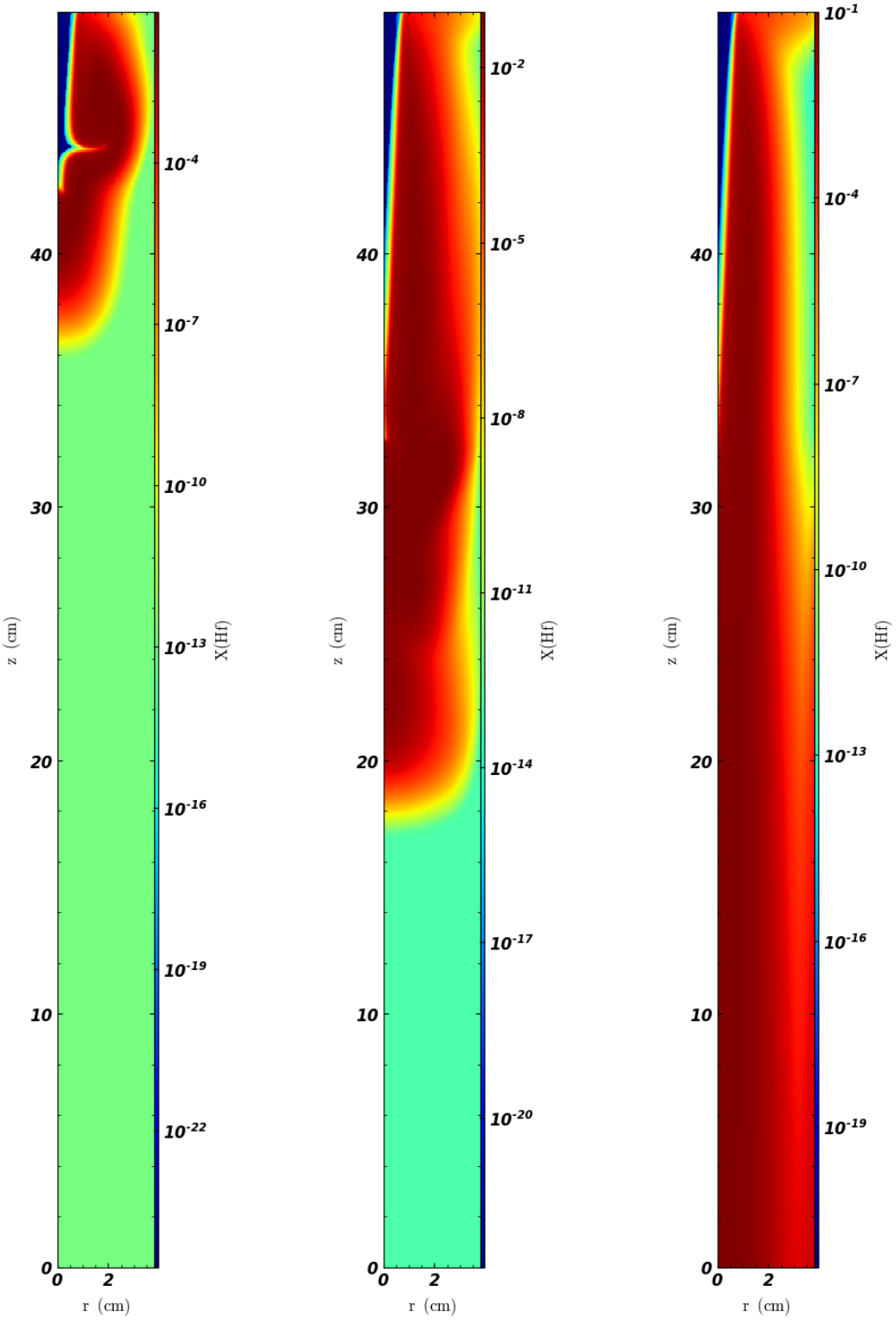

Figure 25: Case 1 - Time evolution of HF molar fraction profile

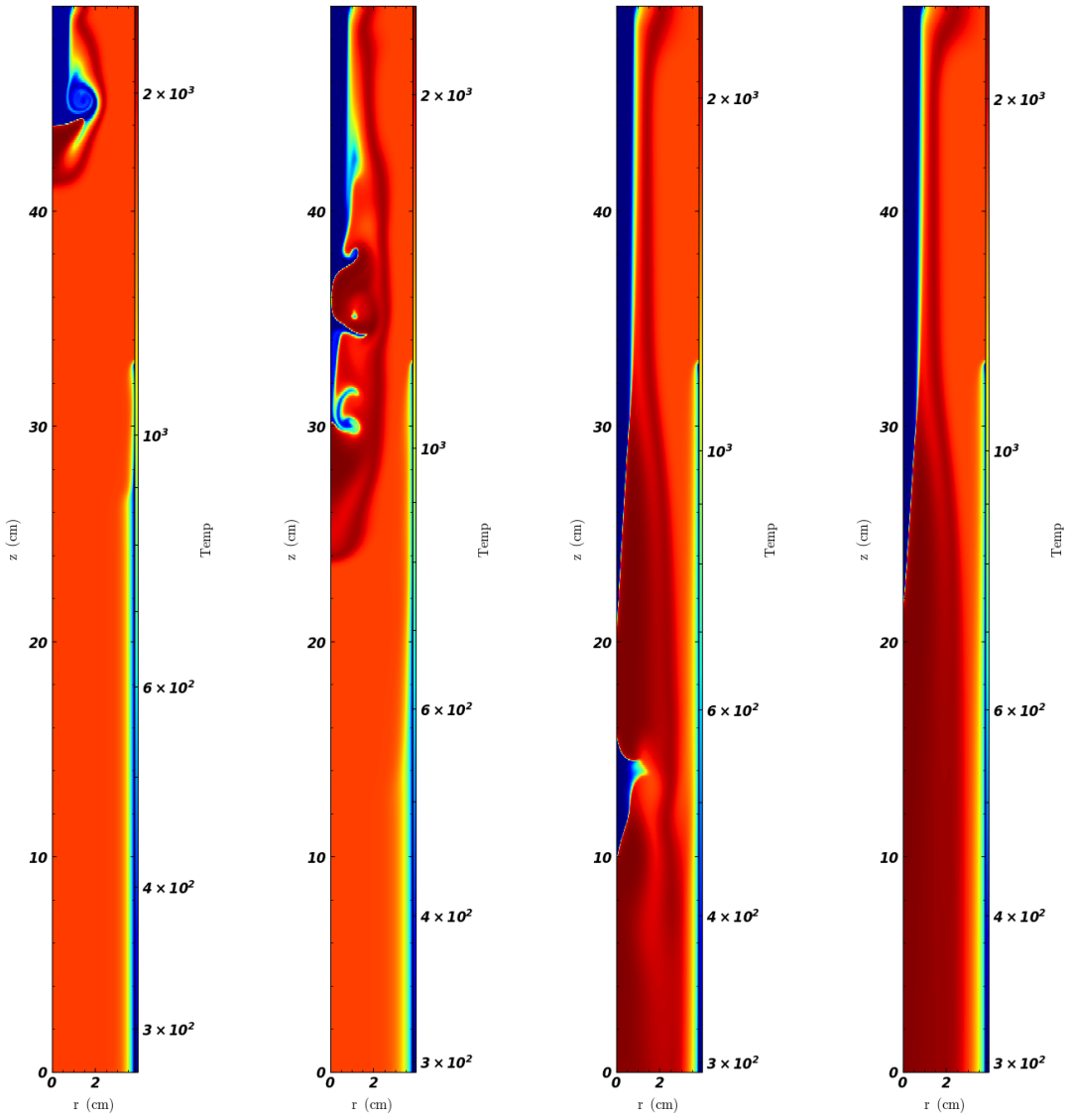

Figure 26: Case 4 - Time evolution of temperature profile

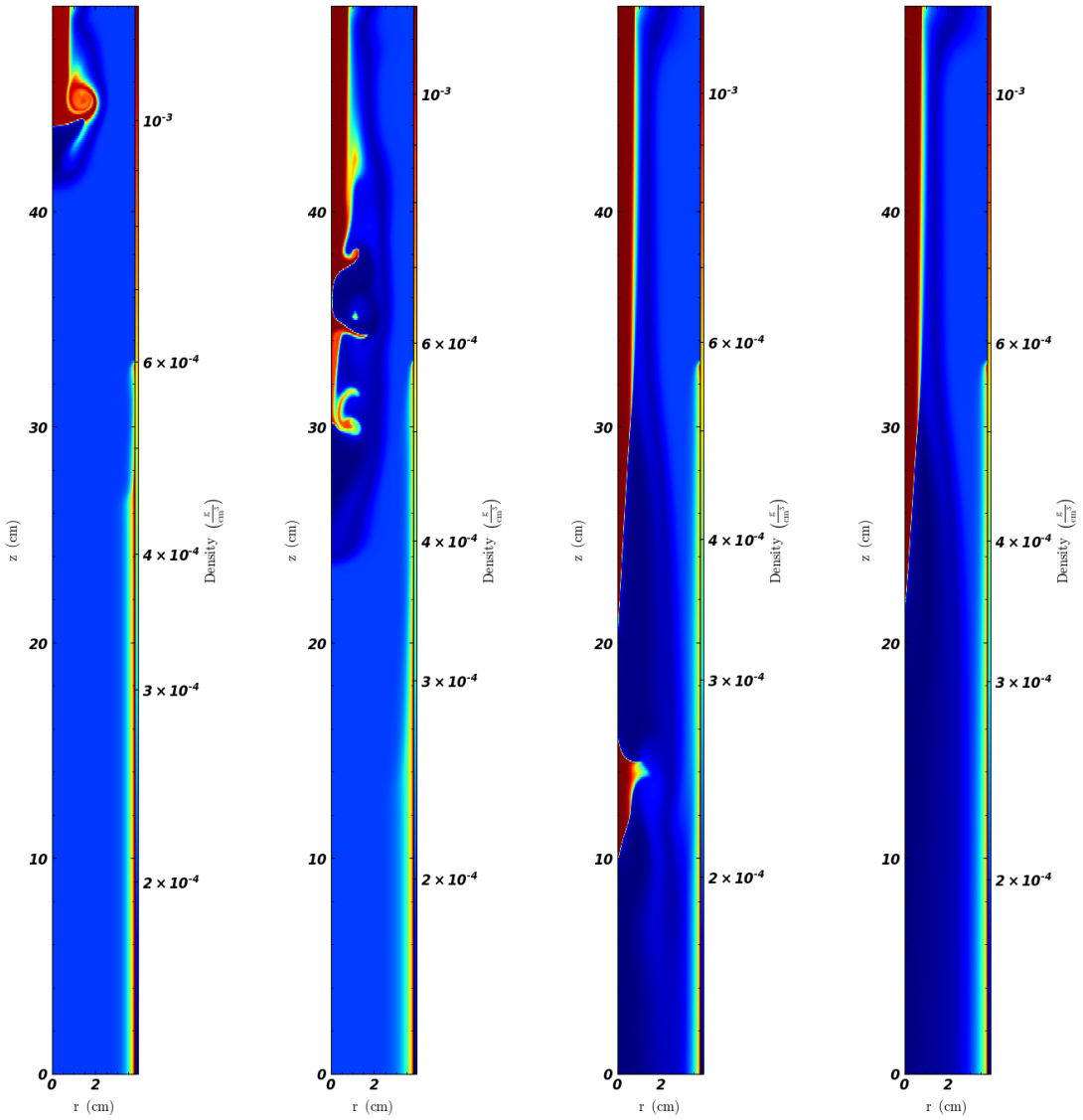

Figure 27: Case 4 - Time evolution of density profile

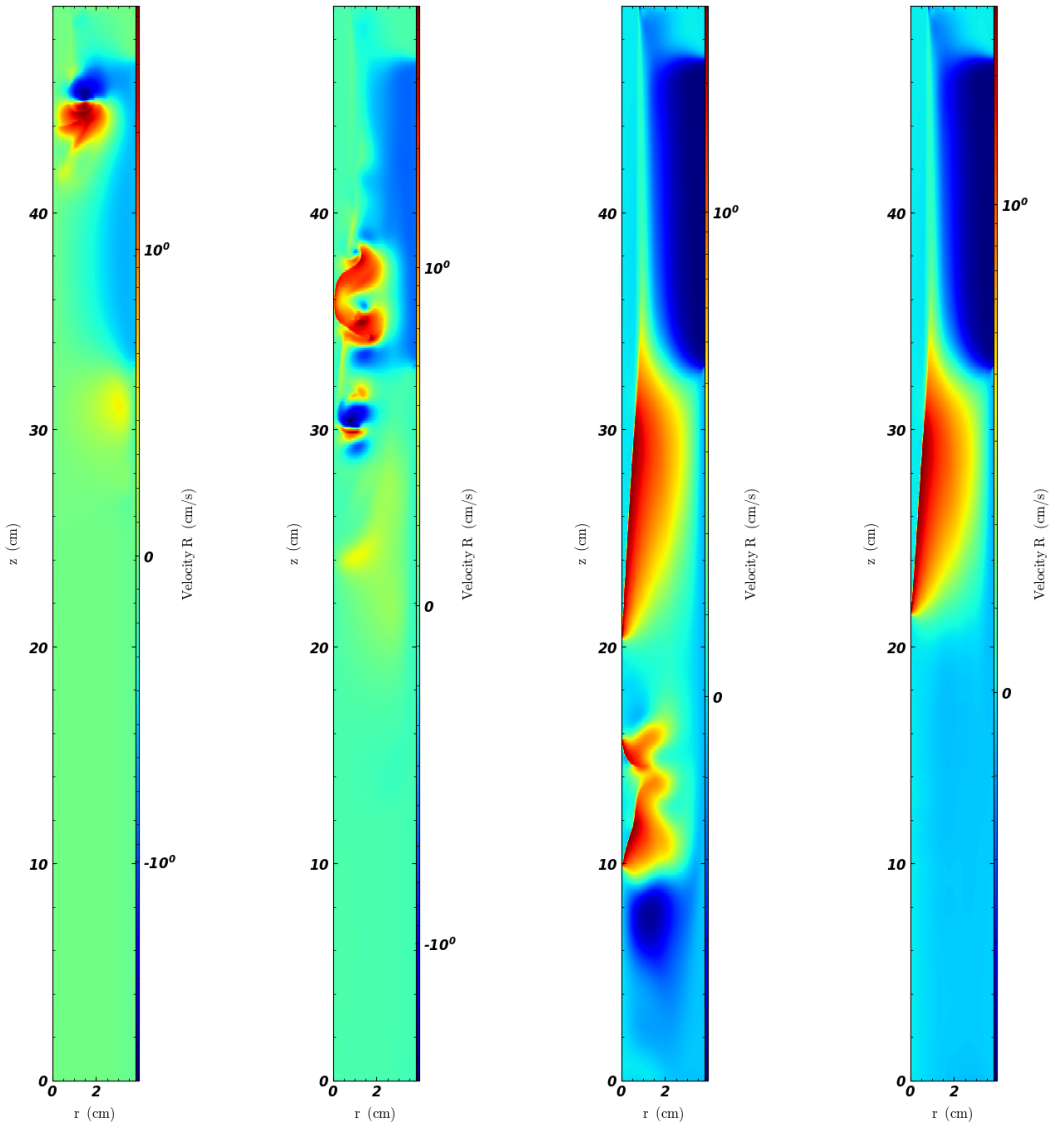

Figure 28: Case 4 - Time evolution of radial velocity profile

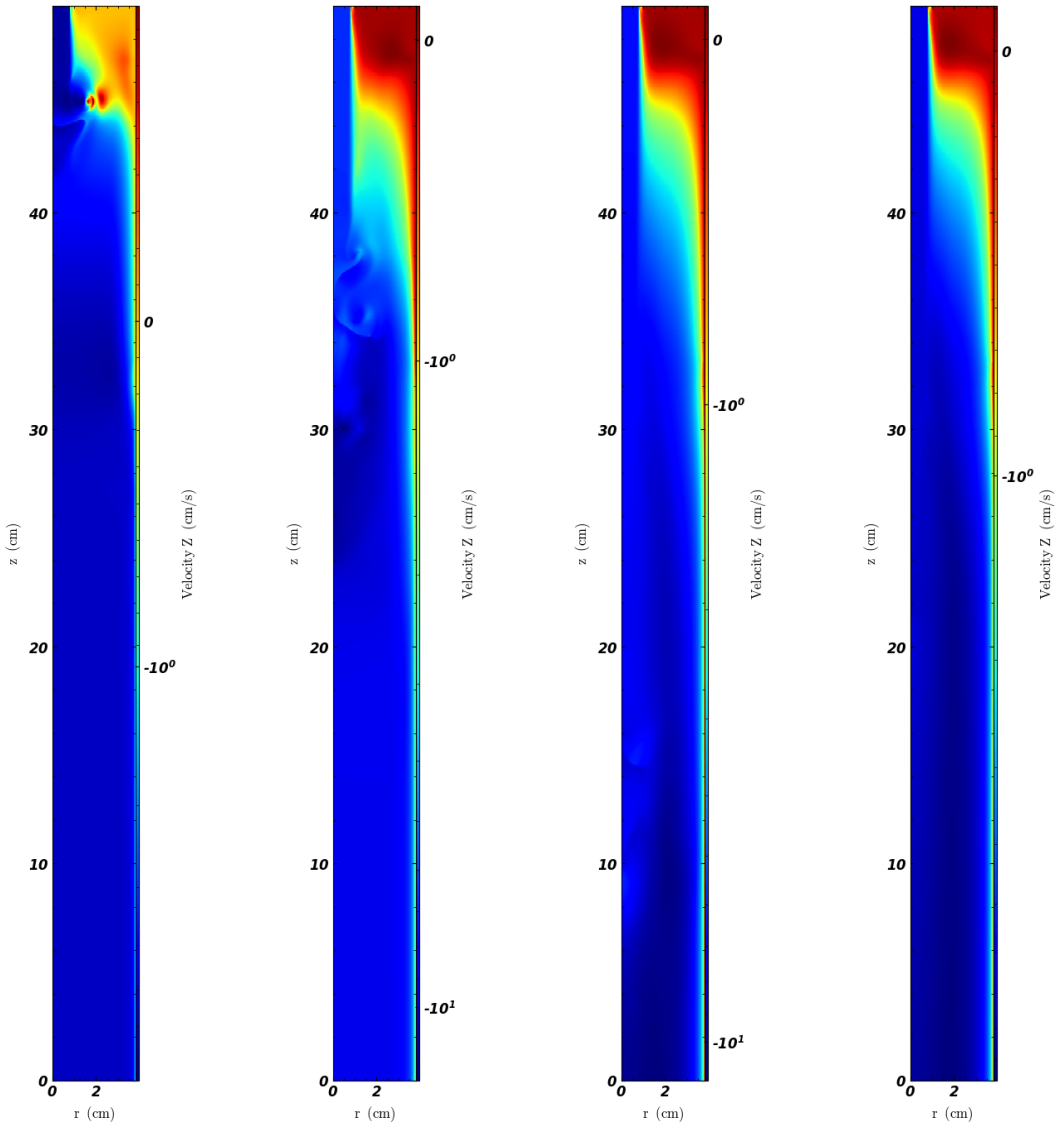

Figure 29: Case 4 - Time evolution of axial velocity profile

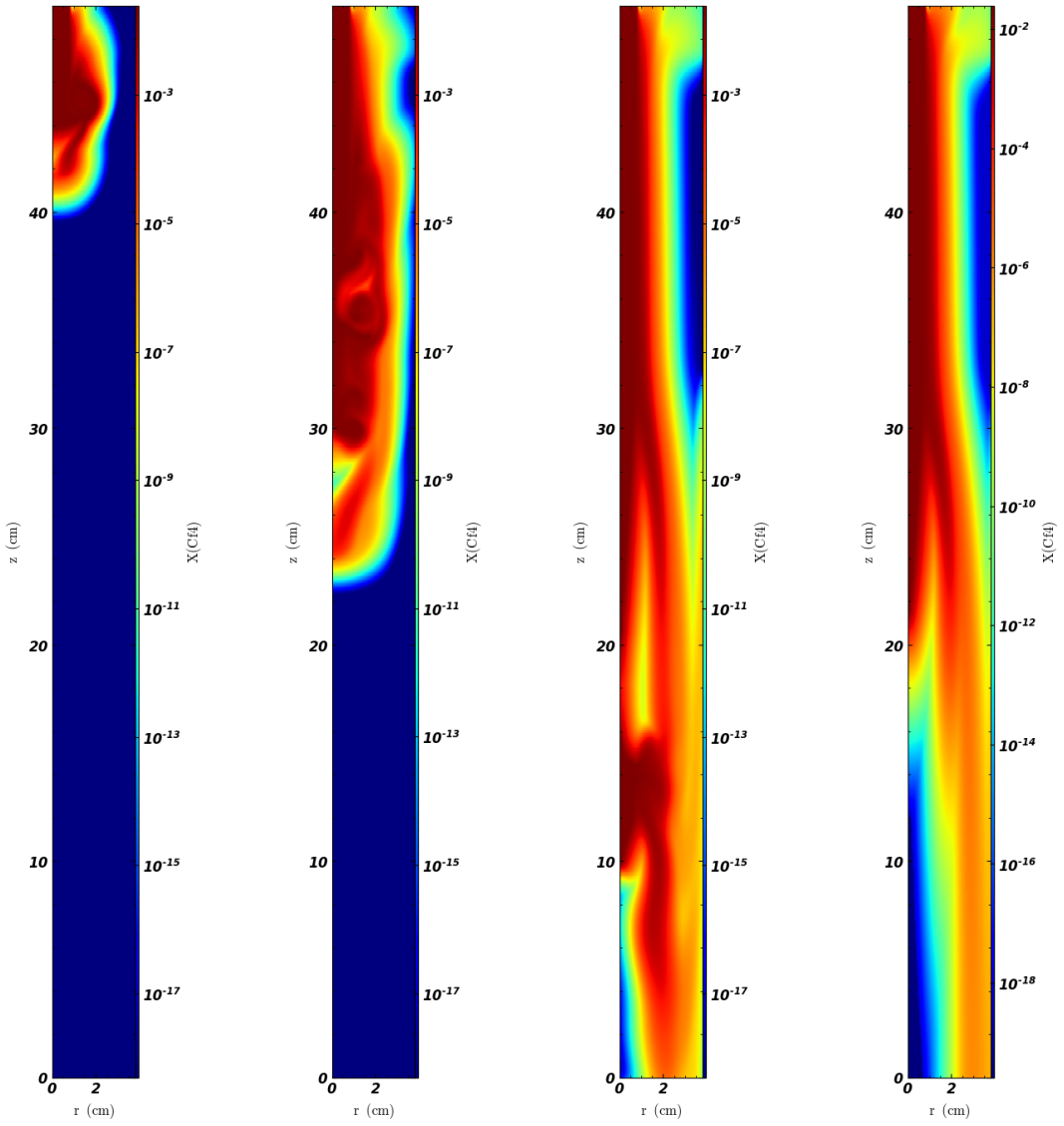

Figure 30: Case 4 - Time evolution of CF_4 molar fraction profile

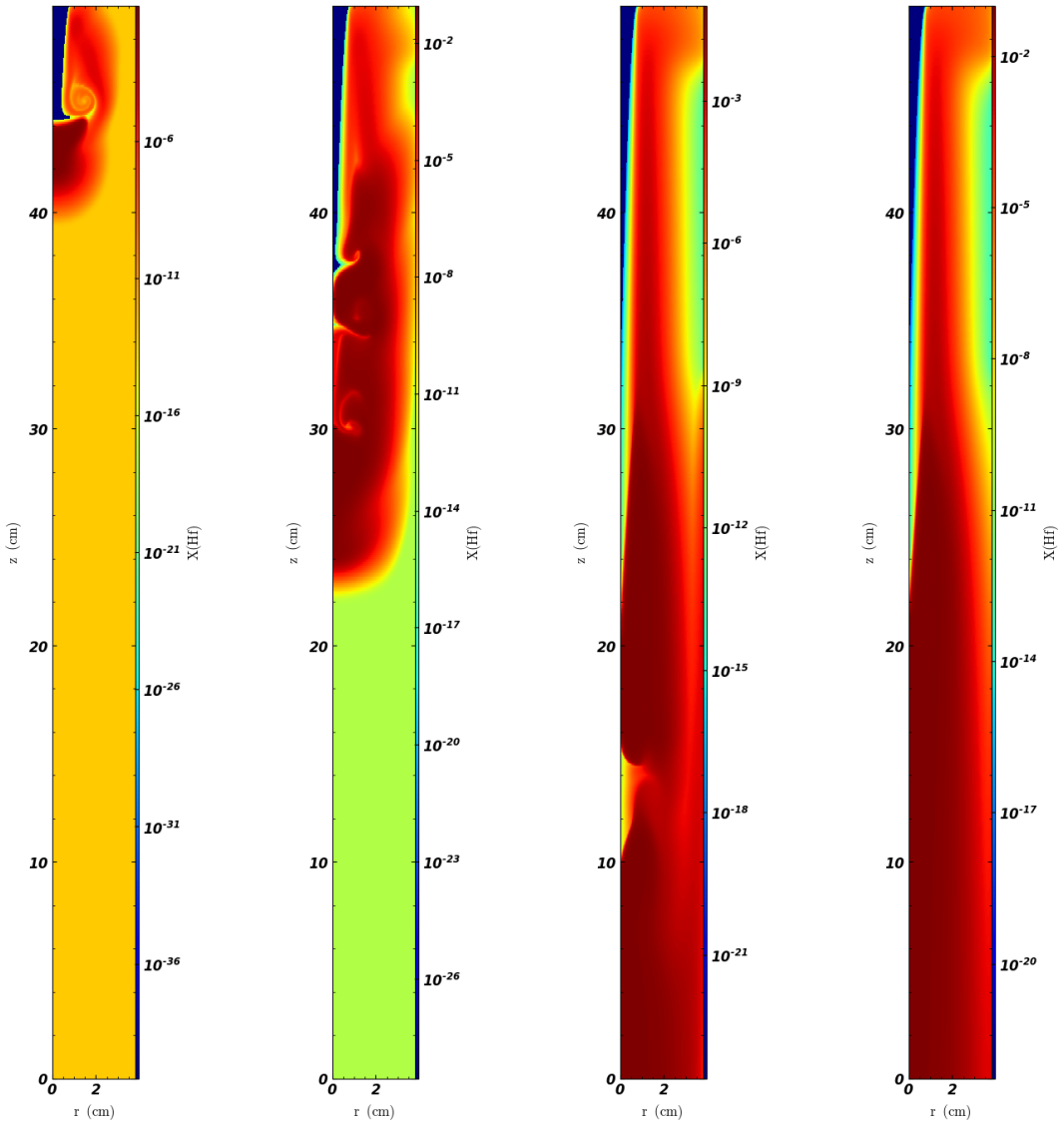

Figure 31: Case 4 - Time evolution of HF molar fraction profile

Test Matrix										
	Baseline	**Vary CH4/O2 Inject (same ratio)**								
Test	1	2	3	4	5					
Values										
Methane Inject	10	12	8	6	4					
Oxygen Inject	18	21.6	14.4	10.8	7.2					
Main Burner Methane	5.375	5.375	5.375	5.375	5.375					
Equivalence Ratio	0.625	0.625	0.625	0.625	0.625					
Adjustment										
Methane Inject	0	20%	-20%	-40%	-60%					
Oxygen Inject	0	20%	-20%	-40%	-60%					
Main Burner Methane	0	0	0	0	0					
Equivalence Ratio	0.625	0.625	0.625	0.625	0.625					
Test Matrix										
	Factorial Design (Vary CH4, O2 2-levels, Methane 3-levels)									
Test	6	7	8	9	10	11	12	13	14	15
Values										
Methane Inject	12	8	12	8	12	8	12	8	8	12
Oxygen Inject	21.6	21.6	14.4	14.4	21.6	21.6	14.4	14.4	21.6	14.4
Main Burner Methane	6.71875	6.71875	6.71875	6.71875	4.03125	4.03125	4.03125	4.03125	5.375	5.375
Equivalence Ratio	0.625	0.625	0.625	0.625	0.625	0.625	0.625	0.625	0.625	0.625
Adjustment										
Methane Inject	20%	-20%	20%	-20%	20%	-20%	20%	-20%	-20%	20%
Oxygen Inject	20%	20%	-20%	-20%	20%	20%	-20%	-20%	20%	-20%
Main Burner Methane	25%	25%	25%	25%	-25%	-25%	-25%	-25%	0%	0%
Equivalence Ratio	0.625	0.625	0.625	0.625	0.625	0.625	0.625	0.625	0.625	0.625

Table 3: List of 1^{st} SET of Case Studies

Test Matrix										
	1.8 Ratio	**Other Ratios**		**Concentric Nozzle**				**Porous Top**		
Test	1	2	3	4	5	6	7	8	9	10
Values										
Methane Inject	7	10	10	10	6	10	10	10	10	10
Oxygen Inject	12.6	16	22	18	18	18	18	18	18	18
Main Burner Methane	5.375	5.375	5.375	5.375	5.375	5.375	5.375	5.375	5.375	5.375
Equivalence Ratio	0.625	0.625	0.625	0.625	0.625	0.625	0.625	0.625	0.625	0.625
Geometry	A	A	A	B	B	B	B	C	C	C
Concentric Nozzle Methane				4	4	2	8			
Porous Top Air								9	18	ϕ=.625
Porous Top Methane								0	0	0.64

Table 4: List of 2^{nd} SET of Case Studies

5.4 Summary of findings and further discussion

- The LBNL code, PeleLM, was used to create simulations of the ALZETA burn-wet CF_4 processing reactor. The code was adjusted to incorporate two rather detailed chemical models of fluorine in the presence of methane combustion. The models were ssembled from a combination of GRI3.0, DRM19 and a NIST database. Based on PeleLM performance characteristics using these models, the chemical descriptions appear to exhibit considerably shorter time scales than the fluid dynamics expected in this low Mach number regime. This "chemical stiffness" leads to substantial difficulty in numerical simuations. PeleLM was used to compute these flows in spite of the numerical difficulties, although consiserable HPC resources were required. To our knowledge, this data could not have been produced by any other approach available.

- Considerable effort early in the project was devoted to characterizing the nature of the chemical system, as modeled with the GRI/DRM/NIST databases. As part of this work, we developed a criteria to use in adaptive simulations that focuses on the chemical processes of interest, rather than a more traditional approach based on spatial resolution of flame and/or fluid features, which are only indirectly related to the objective. Based on this approach we were able to assess the capability of a reduced chemical model as a replacement for the prohibatively expensive one. This pragmatic approach to chemical resolution assessment is of independent scientific interest in our work moving forward.

- On this first pass of the research, ALZETA was interested only in quasi-stationary results from the inherently transient simulation. With no existing steady state flow solver capable of solving this problem, PeleLM was used to generate transient solutions until an approximately steady solution was found. For each case, the resulting "solution" consists of a snapshot containing a set of concentration profiles for 72 chemical species, plus temperature and velocity fields, over the 2d cylindrical computational domain. In order to analyze the detailed chemical system however, complex transformations of this raw data are required which involve the reaction rate expressions, transport properties, thermodynamic relationships, etc. For example, the chemical path analysis, which was summarized earlier in this document, was constructed by using the steady solution state to evaluate instantaneous reaction progress rates over the domain. Those rates were integrated over the computation volume, and collated into fluxes of F atoms moving between chemical species. These types of diagnostics are required to understand and quantify the behavior of the system, but they also hint at the richness of the analysis work yet to do in this area. More complex scenarios would likely increase the volume of data dra-

matically. For example, high-speed and/or time-dependent flow rates into the process inlet may favorably enhance mixing, and possibly turbulence which must be resolved numerically, and analyzed statistically. It is worth noting that our simulations suggest that it may in fact be advantageous to run the system with time-varying inlet conditions, as it may enhance the flame surface density in the device, leading to a more efficient process. Such scenarios were outside the scope of this exploratory study, however.

- The issue of data analysis, even for only the steady solutions, is further complicated by several issues. Practically, there is the need to overcome the hurdle of reading and interpreting the block-structured hierchical adaptive mesh data generated by PeleLM. There is also the complexity of coupling the analysis to tools that are aware of the transformation listed above. Finally, there is the ongoing science of translating physics-based "questions" to ask about the system into quantifyable results and understanding. For example, an engineer may wish to understand the precisely how CF_4 is broken down chemically, and to what extent it is reformed in the reactor. If so, are there distinct regions in space, and/or intermediate chemical compositions that can be altered with auxiliary injection points, so that the reformation is interrupted? As the computational solutions became available in this project, the team was able to begin to address these issues, but little progress has yet been made to extract useful engineering information from the simulation results.
- Although the PeleLM calculations were successful, it is our opinion that the code is likely not currently well-suited for hand-off to ALZETA for the purposes continued independent study. The computational algorithms and data structures in PeleLM are extremely complex, and under these condition, particularly brittle. The code "crashed" often for a variety of reasons, mostly originating from the numerical stiffness of the chemical models, which wer not developed or tuned for time-dependent practical-scale scenarios. Diagnosing and circumventing these failures required considerable expertise not available outside of LBNL.

The above qualifications notwithstanding, this exploratory project has demonstrated to ALZETA that HPC can indeed provide a unique view into their complex engineering problem - one that is simply inaccessible by any other means. The tools allow us to explore the details of the chemical process, and allow one to construct "what-if" scenarios to address shortcomings of the physical device in its current operating modes. However, as with many sources of completely new information, many new questions are illuminated with this capability. It will take considerable time, effort and experience before we learn to probe the solutions, pose operating scenarios and confirm modifications to the device that lead to real engineering advances.

References

[1] A. S. Almgren, J. B. Bell, P. Colella, L. H. Howell, and M. L. Welcome. A Conservative Adaptive Projection Method for the Variable Density Incompressible Navier-Stokes Equations. *Journal of Computational Physics*, 142(1):1–46, 1998.

[2] M. S. Day and J. B. Bell. Numerical simulation of laminar reacting flows with complex chemistry. *Combust. Theory Modelling*, 4:535–556, 2000.

[3] A. Ern and V. Giovangigli. EGLIB: A General-Purpose Fortran Library for Multicomponent Transport Property Evaluations. Technical report, 2004. Version 3.4.

[4] W. Pazner, A. Nonaka, J. Bell, M. Day, and M. Minion. A high-order Spectral Deferred Correction strategy for low Mach number flow with complex chemistry. *Combustion Theory and Modeling*, 3:521–547, 2016.

[5] A. Nonaka, J. Bell, M. Day, C. Gilet, A. Almgren, and M. Minion. A deferred correction coupling strategy for low Mach number flow with complex chemistry. *Combustion Theory and Modeling*, 6:1053–1088, 2012.

[6] G. P. Smith, D. M. Golden, M. Frenklach, N. W. Moriarty, B. Eiteneer, M. Goldenberg, R. K. Bowman, C. T. an d Hanson, S. Song, W. C. Gardiner Jr., V. V. Lissianski, and Z. Qin. GRI-Mech 3.0. `http://www.me.berkeley.edu/gri_mech/`.

[7] Jr. D.R. Burgess, M.R. Zachariah, W. Tsang, and P.R. Westmoreland. Thermochemical and chemical kinetic data for fluorinated hydrocarbons. *Prog. Energy Combust. Sci.*, 21:453–529, 1996.

[8] M. J. Turk, B. D. Smith, J. S. Oishi, S. Skory, S. W. Skillman, T. Abel, and M. L. Norman. yt: A Multi-code Analysis Toolkit for Astrophysical Simulation Data. *The Astrophysical Journal Supplement Series*, 192:9, January 2011.